

## OPTIMALLY ACCURATE HIGHER-ORDER FINITE ELEMENT METHODS FOR POLYTOPIAL APPROXIMATIONS OF DOMAINS WITH SMOOTH BOUNDARIES

JAMES CHEUNG, MAURO PEREGO, PAVEL BOCHEV, AND MAX GUNZBURGER

**ABSTRACT.** Meshing of geometric domains having curved boundaries by affine simplices produces a polytopial approximation of those domains. The resulting error in the representation of the domain limits the accuracy of finite element methods based on such meshes. On the other hand, the simplicity of affine meshes makes them a desirable modeling tool in many applications. In this paper, we develop and analyze higher-order accurate finite element methods that remain stable and optimally accurate on polytopial approximations of domains with smooth boundaries. This is achieved by constraining a judiciously chosen extension of the finite element solution on the polytopial domain to weakly match the prescribed boundary condition on the true geometric boundary. We provide numerical examples that highlight key properties of the new method and that illustrate the optimal  $H^1$ - and  $L^2$ -norm convergence rates.

### 1. INTRODUCTION

It is well known that standard finite element methods based on piecewise polynomials of degree greater than one do not achieve optimal accuracy whenever a domain  $\Omega$  having a curved boundary is approximated by a polygonal or polyhedral domain  $\Omega_h$ . Table 1 illustrates this fact for finite element approximations of a smooth solution of the Poisson equation on the unit disc approximated by inscribed regular polygons with sides of length  $h$ . The table shows that in all cases the  $L^2(\Omega_h)$ -norm convergence rate is capped at approximately 2 whereas the  $H^1(\Omega_h)$ -norm convergence rate is approximately 3/2. Of course, the explanation for such loss of precision is also well known: the approximation theoretic convergence rates for higher-degree polynomials are swamped by the geometric error of  $O(h^2)$  resulting from defining the finite element discretization on the approximate domain  $\Omega_h$  instead of the true domain  $\Omega$ , including imposing the boundary condition on the boundary  $\Gamma_h$  of  $\Omega_h$  instead of on the exact boundary  $\Gamma$  of  $\Omega$ . This loss of accuracy is an example of a *variational crime* [28, Chapter 4, p. 172] and has nothing to do with the regularity of the exact solution; indeed, the loss occurs for  $C^\infty(\overline{\Omega})$  and even analytic exact solutions.

---

Received by the editor February 8, 2018, and, in revised form, October 28, 2018.

2010 *Mathematics Subject Classification*. Primary 65N30.

Sandia National Laboratories is a multimission laboratory managed and operated by National Technology and Engineering Solutions of Sandia, LLC., a wholly owned subsidiary of Honeywell International, Inc., for the U.S. Department of Energy's National Nuclear Security Administration under contract DE-NA-0003525.

This material is based upon work supported by the U.S. Department of Energy, Office of Science, Office of Advanced Scientific Computing Research. Additionally, the first and fourth authors were supported by US Department of Energy grant DE-SC0009324 and US Air Force Office of Scientific Research grant FA9550-15-1-0001.

TABLE 1. Finite element convergence rates for smooth solutions of a Poisson equation on the unit disk approximated by a sequence of regular inscribed polygons with side length  $h$ . The last row shows the theoretical convergence rate of the best approximation (BA) out of each finite element space.

Element type	Quadratic		Cubic		Quartic	
Error type	$L^2(\Omega_h)$	$H^1(\Omega_h)$	$L^2(\Omega_h)$	$H^1(\Omega_h)$	$L^2(\Omega_h)$	$H^1(\Omega_h)$
Convergence rate	2.188	1.698	2.115	1.590	2.151	1.590
BA rate	3.0	2.0	4.0	3.0	5.0	4.0

In this paper, we develop and analyze a new finite element formulation that remains, under certain assumptions, optimally accurate for finite element spaces of arbitrary orders defined on polytopal approximations of geometric domains with smooth boundaries. The significance of this work stems from the fact that finite element methods based on affine simplicial grids remain one of the most efficient instances of this class of methods, both in terms of mesh generation and computational costs. For example, an affine simplex has a constant Jacobian determinant that can be precomputed, thereby allowing significant savings in the application of various pullbacks necessary for, e.g., compatible finite elements. Yet, because the resulting polytopal approximation of the geometric domain is only at best second-order accurate, such meshes create an accuracy bottleneck for higher-order elements. Overcoming this bottleneck is the main purpose of this paper.

To put our work in a proper context, we briefly discuss relevant mesh types and survey related existing literature.

**Simplicial mesh types.** Meshing of a domain  $\Omega$  with curved boundaries by affine simplices yields a polytopal approximation  $\Omega_h$  of the former, where  $\Omega_h$  is the union of all the simplices. In many practical cases, all vertices on the approximate boundary  $\Gamma_h$  lie on the exact boundary  $\Gamma$ . We refer to such meshes as *Type A meshes*. Alternately, for a *Type B mesh*, none or at least not all of the vertices of  $\Gamma_h$  lie on  $\Gamma$ . The simplest examples of Types A and B meshes are inscribed and circumscribed polygons for a disk, respectively. For a Type A mesh the distance between the boundaries of  $\Omega$  and  $\Omega_h$  is of order  $O(h^2)$ , where  $h$  is a measure of the size of the finite element grid cells. For Type B meshes, this distance can be larger than  $O(h^2)$ . In this work we restrict attention to Type A meshes and Type B meshes for which the distance between the discrete and continuous boundaries is of order  $O(h^2)$ .

**Existing work.** There are two fundamentally different strategies for achieving optimal error bounds for high-order elements on curved domains. The first focuses on reducing the geometric approximation error in  $\Omega_h$  without modifying the underlying variational formulation for the finite element method. A classical example of this idea is the isoparametric finite element method [17] that maps reference elements to curvilinear elements using carefully chosen polynomial transformations of the same degree as that of the finite element space. The work in [23] introduces a method for generating isoparametric maps for curved domains of any dimension that has the property of preserving the optimality of the underlying polynomial approximation space.

Another example of the first strategy is the isogeometric analysis approach (IGA) [15, 21] that uses nonuniform rational B-splines (NURBS) as a finite element basis and achieves optimal accuracy for curved domains. IGA generates a mesh of control points for the NURBS basis and then applies a transformation map to the control points to obtain a highly accurate approximation  $\Omega_h$  of the curved domain  $\Omega$ . However, the NURBS basis makes the IGA approach more difficult to implement and more costly to solve than traditional polynomial-based finite elements. Other notable methods in this category are the NURBS enhanced finite element method [27], and the recently developed virtual element method for curved boundaries [3].

The second, less explored, strategy retains the polytopial domain approximation but modifies the underlying variational problem in order to compensate for the fixed geometric error in  $\Omega_h$ . For example, optimal error estimates are obtained in [12–14] for Type B meshes by using polynomial extensions and line integrals to transfer Dirichlet boundary values from the curved boundary  $\Gamma$  to the approximate boundary  $\Gamma_h$ . The primary difficulties of this approach include the construction of line integrals and the additional expense incurred because of the use of the hybridized discontinuous Galerkin method on mixed formulations of elliptic PDEs. Another example is found in [22], where optimal higher-order convergence rates were demonstrated numerically for the Euler equations by using the normal vectors of curved domains instead of the approximate normal vectors to enforce a no-penetration condition on Type A meshes.

Recently, in [24, 25], a method was developed that achieves optimal error convergence for piecewise linear elements on Type B meshes for Dirichlet elliptic boundary-value problems. A linear extension is constructed to weakly match the boundary conditions by using the Nitsche method. Optimal  $H^1$ -norm and  $L^2$ -norm convergence rates are demonstrated even if the distance between the computational and the actual boundaries is  $O(h)$ . Optimal  $H^1$ -norm convergence rates were derived through a theoretical analysis.

Another similar method was presented in [6], where a Taylor series expansion in the normal direction with respect to a background Type B cut-mesh is used to provide a boundary value correction for Dirichlet problems posed on curved domains. The extension terms are again enforced using a Nitsche method, and optimal  $H^1$ -norm and  $L^2$ -norm convergence rates were derived theoretically and the numerical computations confirm their theoretical findings.

**What is new in this paper.** Our new approach is an example of the second strategy, i.e., it relies on suitable modifications of the variational formulation when defining the finite element method in order to recover optimal convergence rates on polytopial approximations of curved domains. The method is applicable to both Dirichlet and Neumann boundary conditions. In a nutshell, it forces a polynomial extension of the approximate solution to match the prescribed boundary condition data on the boundary of the given domain  $\Omega$ ; thus, we refer to this approach as the *polynomial extension finite element method* (PE-FEM). The extended Dirichlet condition is weakly enforced whereas the extended Neumann condition is enforced as a natural condition for a modified weak formulation of the boundary-value problem. We prove stability and optimal  $H^1(\Omega_h)$  accuracy for both the Dirichlet and Neumann problems and show that, on convex meshes and under additional regularity assumptions, the former also converges optimally in  $L^2(\Omega_h)$ . Furthermore, computational studies indicate that optimal  $L^2(\Omega_h)$ -norm convergence is also achieved

for the Neumann problem. In addition to recovering optimal accuracy, the method is computationally efficient and simple to implement. The ideas presented in this paper were first explored in the context of interface problems with geometrically nonmatching discrete interfaces in [7]. Conversely, results of this work have been applied to the analysis of such interface problems in [8].

Unlike previous works, our Dirichlet approximation does not require the use of a stabilized Nitsche formulation. This is significant in practice because the choice of the stabilization term's value is inherently linked to the well-posedness of the discrete problem; i.e., it must be chosen large enough to ensure coercivity of the bilinear form while also small enough to minimize its effect on the conditioning of the algebraic system. We also provide a theoretical stability and convergence analysis for the Neumann problem, whereas previous works focus almost entirely on the Dirichlet problem. Implicit in the analysis in previous works is the assumption that the classical Taylor theorem applies to functions in Sobolev spaces. By using instead an averaged Taylor series extension we are able to forgo this assumption and obtain discrete formulations that are meaningful for functions in  $W_p^m$  spaces.

The paper is organized as follows. Section 2 introduces the necessary technical background. In §3, we describe the PE-FEM Dirichlet and Neumann formulations and then, in §4.1, we prove the well-posedness of the discretized problems. Then, in §4.3, we derive optimal error estimates with respect to the  $L^2(\Omega_h)$ - and  $H^1(\Omega_h)$ -norms for the Dirichlet problem and the optimal  $H^1(\Omega_h)$ -norm error bounds for the Neumann problem. To streamline the flow of the paper, we relegate long proofs to the appendices. In §5, we discuss some implementation issues attendant to the PE-FEM and, in §6, we provide illustrative numerical results for the PE-FEM based on Type A meshes. Concluding remarks are provided in §7.

## 2. PRELIMINARIES

Let  $k = 2, 3, \dots$  and let  $\Omega \subset \mathbb{R}^N$ ,  $N = 2, 3$ , denote a bounded, open domain having a  $C^{k+1}$  boundary  $\Gamma$  with  $\mathbf{n}$  denoting the outer unit normal vector. We consider approximations of  $\Omega$  by affine simplicial meshes  $\Omega_h$ , i.e., collections of open  $N$ -simplices  $\{\mathcal{K}_j\}$  such that the nonempty intersections of their closures consist of only vertices, complete edges, or complete faces. Here  $h := \max_{\mathcal{K}_j \in \Omega_h} \text{diam}(\mathcal{K}_j)$  denotes the mesh size parameter. Every mesh  $\Omega_h$  defines a polytopial approximation of  $\Omega$ , which we also denote by  $\Omega_h$ ; see Figure 1 for a two-dimensional illustration. We note that the boundary  $\Gamma_h$  of  $\Omega_h$  is a union of  $(N-1)$ -simplices  $\{\mathcal{E}_i\}$  so that the outer unit normal vector  $\mathbf{n}_h$  to  $\Gamma_h$  is in general a piecewise constant vector field and is thus only piecewise continuous. For every  $\mathcal{E}_i \in \Gamma_h$ , let  $\mathcal{K}_{j_i}$  denote the element of  $\Omega_h$  whose closure contains  $\mathcal{E}_i$  on its boundary. Throughout,  $C$  denotes a positive constant whose value changes from one instance to another but which does not depend on  $h$ .

It follows from the smoothness assumption made about  $\Gamma$  that, for every  $\mathcal{E}_i \in \Gamma_h$ , there exists a  $C^{k+1}(\overline{\mathcal{E}}_i)$  mapping  $\boldsymbol{\eta}_i : \mathcal{E}_i \rightarrow \Gamma$  such that  $\boldsymbol{\eta}_i(\boldsymbol{\xi}) \in \Gamma$  for every  $\boldsymbol{\xi} \in \mathcal{E}_i$  and such that

$$(1) \quad \max_{\mathcal{E}_i \in \Gamma_h} \sup_{\boldsymbol{\xi} \in \mathcal{E}_i} |\boldsymbol{\eta}_i(\boldsymbol{\xi}) - \boldsymbol{\xi}| \leq \delta_h$$

for some  $\delta_h \in \mathbb{R}^+$ , where  $|\cdot|$  denotes the Euclidean norm. The mappings  $\boldsymbol{\eta}_i$  define a piecewise  $C^{k+1}$  map  $\boldsymbol{\eta} : \Gamma_h \rightarrow \Gamma$ . The value of  $\delta_h$  in (1) can be viewed as a measure of the geometric error in the approximation of  $\Omega$  by  $\Omega_h$ . See the left sketch in

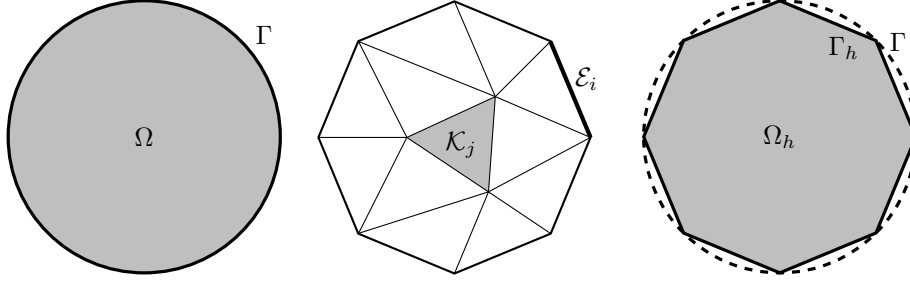


FIGURE 1. A curved domain  $\Omega$  (left), an associated affine simplicial mesh  $\Omega_h$  (center), and the resulting polygonal approximation  $\Omega_h$  (right).

Figure 2 for an illustration. The right sketch of Figure 2 illustrates the pullback from  $\Gamma$  to  $\Gamma_h$ , i.e., how the value of a function  $v(\boldsymbol{\eta})$  evaluated at a point  $\boldsymbol{\eta}_i \in \Gamma$  is pulled back to the point  $\boldsymbol{\xi} \in \mathcal{E}_i \subset \Gamma_h$ .

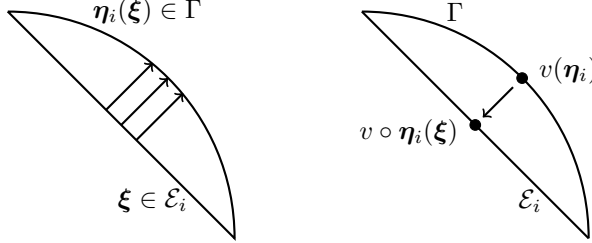


FIGURE 2. Left: An example of a  $C^{k+1}$  mapping  $\boldsymbol{\eta}_i : \mathcal{E}_i \rightarrow \Gamma$  defined as the intersection of a line normal to  $\mathcal{E}_i$  with the true boundary  $\Gamma$ . Right: A sketch of a pullback from the continuous boundary onto the polygonal boundary.

Let  $\boldsymbol{\alpha} = (\alpha_n)_{n=1}^N$ ,  $\alpha_n$  a nonnegative integer, denote a multi-index and let  $|\boldsymbol{\alpha}| = \sum_{n=1}^N \alpha_n$  and  $\boldsymbol{\alpha}! = \prod_{n=1}^N \alpha_n!$ . For  $\mathcal{D} = \Omega$  or  $\Omega_h$  and for  $m \in \mathbb{N}$ , let  $H^m(\mathcal{D})$  denote the standard Sobolev space and  $(H^m(\mathcal{D}))'$  the corresponding dual space; see [1]. Also, for any  $\boldsymbol{\xi} \in \mathbb{R}^N$ , let  $\boldsymbol{\xi}^\boldsymbol{\alpha} := \xi_1^{\alpha_1} \xi_2^{\alpha_2} \cdots \xi_N^{\alpha_N}$  and  $D^\boldsymbol{\alpha} := \partial^{|\boldsymbol{\alpha}|} / \partial^{\alpha_1} \xi_1 \partial^{\alpha_2} \xi_2 \cdots \partial^{\alpha_N} \xi_N$ . For  $\mathcal{D} = \Gamma$  or  $\Gamma_h$ , we consider the fractional Sobolev space  $H^{m-\frac{1}{2}}(\mathcal{D})$ . The  $k$ th order Lagrange finite element space is defined by

$$V_h^k := \{v \in C^0(\overline{\Omega}_h) : v|_{\mathcal{K}_j} \in P_k(\mathcal{K}_j) \quad \forall \mathcal{K}_j \in \Omega_h\} \subset H^1(\Omega_h),$$

where  $P_k(\mathcal{K}_j)$  denotes the space of polynomials of degree at most  $k$  defined over the  $N$ -simplex  $\mathcal{K}_j \subset \mathbb{R}^N$ . In addition, we have the constrained space

$$V_{h,0}^k := \{v \in V_h^k : v = 0 \text{ on } \Gamma_h\} \subset H_0^1(\Omega_h)$$

and the trace space

$$W_h^k := V_h^k|_{\Gamma_h} = \{v \in C^0(\Gamma_h) : v|_{\mathcal{E}_i} \in P_k(\mathcal{E}_i) \quad \forall \mathcal{E}_i \in \Gamma_h\} \subset H^{1/2}(\Gamma_h).$$

We also define the discontinuous finite element space

$$\overline{V}_h^k := \{v \in L^2(\Omega_h) : v|_{\mathcal{K}_j} \in P_k(\mathcal{K}_j) \quad \forall \mathcal{K}_j \in \Omega_h\}$$

and the discrete differential operator  $D_h^\alpha : \overline{V}_h^k \rightarrow L^2(\overline{\Omega}_h)$  defined by

$$D_h^\alpha v_h(\mathbf{x}) := \begin{cases} D^\alpha v_h(\mathbf{x}) & \text{if } \mathbf{x} \in \mathcal{K}_j \text{ for } \mathcal{K}_j \in \Omega_h, \\ 0 & \text{otherwise.} \end{cases}$$

Duality pairings over  $\Omega_h$  and  $\Gamma_h$  are defined by

$$\langle v, w \rangle_{\Omega_h} = \sum_{\mathcal{K}_j \in \Omega_h} \int_{\mathcal{K}_j} v w d\mathcal{K}_j \quad \text{and} \quad \langle v, w \rangle_{\Gamma_h} = \sum_{\mathcal{E}_i \in \Gamma_h} \int_{\mathcal{E}_i} v w d\mathcal{E}_i,$$

respectively. ‘‘Broken’’ Sobolev norms on  $\Omega_h$  and  $\Gamma_h$  are defined by

$$\|v\|_{m,\Omega_h}^2 = \sum_{\mathcal{K}_j \in \Omega_h} \|v\|_{m,\mathcal{K}_j}^2 \quad \forall v \in V_h^k \quad \text{and} \quad \|w\|_{m,\Gamma_h}^2 = \sum_{\mathcal{E}_i \in \Gamma_h} \|w\|_{m,\mathcal{E}_i}^2 \quad \forall w \in W_h^k,$$

respectively. On the discrete spaces  $V_h^k$  and  $W_h^k$  we have the inverse inequalities involving the corresponding ‘‘broken’’ norms given by

$$\|v\|_{m,\Omega_h} \leq Ch^{-1} \|v\|_{m-1,\Omega_h} \quad \forall v \in V_h^k, \quad m = 1, 2, \dots,$$

and

$$\|w\|_{m+1/2,\Gamma_h} \leq Ch^{-\frac{1}{2}} \|w\|_{m,\Gamma_h} \quad \forall w \in W_h^k, \quad m = 0, 1, \dots.$$

The smoothness assumption on  $\Gamma$  implies the existence of a continuous lifting operator  $\mathcal{R}(\cdot) : H^{k+1/2}(\Gamma) \rightarrow H^{k+1}(\Omega)$  such that for all  $g \in H^{k+1/2}(\Gamma)$  there exists  $v = \mathcal{R}(g) \in H^{k+1}(\Omega)$  with  $\|v\|_{k+1,\Omega} \leq C_{\mathcal{R}} \|g\|_{k+\frac{1}{2},\Gamma}$ . We also have the continuous discrete lifting operator  $\mathcal{R}_h(\cdot) : W_h^k \rightarrow V_h^k$  such that for all  $g_h \in W_h^k$  there exists  $v_h = \mathcal{R}_h(g_h) \in V_h^k$  with  $\|v_h\|_{k+1,\Omega_h} \leq C_{\mathcal{R}_h} \|g_h\|_{k+\frac{1}{2},\Gamma_h}$ .

Finally we recall the approximation theoretic bound

$$(2) \quad \inf_{\chi \in V_h^k} \|v - \chi\|_{s,\Omega_h} \leq Ch^{k-s+1} |v|_{k+1,\Omega_h} \quad \text{for } s = 0, 1 \text{ and } \forall v \in H^{k+1}(\Omega_h)$$

that holds under the assumption that  $\Omega_h$  is a regular mesh [9].

**2.1. Setting.** To present the key ideas of the method without unnecessary technical complications we consider the Dirichlet problem

$$(3) \quad -\nabla \cdot (p(\mathbf{x}) \nabla u) = f \quad \text{on } \Omega \quad \text{and} \quad u = g_D \quad \text{on } \Gamma$$

and the Neumann problem

$$(4) \quad -\nabla \cdot (p(\mathbf{x}) \nabla u) + q(\mathbf{x}) u = f \quad \text{in } \Omega \quad \text{and} \quad p \nabla u \cdot \mathbf{n} = g_N \quad \text{on } \Gamma.$$

Here,  $p, q \in C^k(\overline{\Omega})$ ,  $g_D(\mathbf{x}) \in H^{k+1/2}(\Gamma)$ ,  $g_N(\mathbf{x}) \in H^{k-1/2}(\Gamma)$ , and  $f \in H^{k-1}(\Omega)$  are given functions such that  $\underline{p} \leq p(\mathbf{x}) \leq \bar{p}$  for some  $\underline{p} > 0$  and  $\bar{p} < \infty$  and  $q(\mathbf{x}) > 0$ .<sup>1</sup>

A weak formulation of (3) seeks  $u \in H^1(\Omega)$  such that

$$(5) \quad D(u, v) = \langle f, v \rangle_\Omega \quad \forall v \in H_0^1(\Omega) \quad \text{and} \quad u = g_D \text{ on } \Gamma$$

whereas a weak formulation of (4) seeks  $u \in H^1(\Omega)$  such that

$$(6) \quad N(u, v) = \langle f, v \rangle_\Omega + \langle g_N, v \rangle_\Gamma \quad \forall v \in H^1(\Omega),$$

---

<sup>1</sup>The last assumption obviates the need to work in the quotient space  $H^1(\Omega) \setminus \mathbb{R}$  for the Neumann problem.

where the bilinear forms  $D(\cdot, \cdot) : H^1(\Omega) \times H^1(\Omega) \rightarrow \mathbb{R}$  and  $N(\cdot, \cdot) : H^1(\Omega) \times H^1(\Omega) \rightarrow \mathbb{R}$  are defined by

$$D(u, v) := \int_{\Omega} p \nabla u \cdot \nabla v \, d\mathbf{x} \quad \text{and} \quad N(u, v) := \int_{\Omega} (p \nabla u \cdot \nabla v + q u v) \, d\mathbf{x},$$

respectively. Both (5) and (6) are well-posed for  $f \in H^{-1}(\Omega)$ ,  $g_D \in H^{1/2}(\Gamma)$ , and  $g_N \in H^{-1/2}(\Gamma)$ , whereas our regularity assumptions on  $\Gamma$ ,  $g_D$ ,  $g_N$ ,  $p$ ,  $q$ , and  $f$  imply that  $u \in H^{k+1}(\Omega)$ .

In general,  $\Omega_h \not\subset \Omega$  and  $\Omega \not\subset \Omega_h$ ; see Figure 3 for an illustration. As a result, if  $\Omega_h \not\subset \Omega$ , the data  $p$ ,  $q$ , and  $f$  and the solution  $u$  of (3) or (4) may not be defined on all of  $\Omega_h$  so that extensions of these functions from  $\Omega$  to  $\Omega \cup \Omega_h$  are required. Our regularity assumptions imply the existence of bounded extensions<sup>2</sup>  $\tilde{p} \in C^k(\mathbb{R}^N)$ ,  $\tilde{q} \in C^k(\mathbb{R}^N)$ ,  $\tilde{f} \in H^{k-1}(\mathbb{R}^N)$ , and  $\tilde{u} \in H^{k+1}(\mathbb{R}^N)$  such that  $\tilde{p} = p$ ,  $\tilde{q} = q$ ,  $\tilde{u} = u$ , and, for  $k \geq 1$ ,  $\tilde{f} = f$  almost everywhere in  $\Omega$ . For  $k = 0$ , we have  $\langle \tilde{f}, v \rangle_{\Omega} = \langle f, v \rangle_{\Omega}$  for all  $v \in H^1(\Omega)$ . In particular, there exist extensions such that  $\|\tilde{u}\|_{k+1, \Omega \cup \Omega_h} \leq C_e \|u\|_{k+1, \Omega}$ ,  $\|\tilde{f}\|_{k-1, \Omega \cup \Omega_h} \leq C_e \|f\|_{k-1, \Omega}$ ,  $\|\tilde{p}\|_{C^k(\overline{\Omega \cup \Omega_h})} \leq C_e \|p\|_{C^k(\overline{\Omega})}$ , and  $\|\tilde{q}\|_{C^k(\overline{\Omega \cup \Omega_h})} \leq C_e \|q\|_{C^k(\overline{\Omega})}$  for a constant  $C_e > 0$  having value independent of  $u$ ,  $f$ ,  $p$ , or  $q$ .

### 3. THE PE-FEM

We now introduce the *polynomial extension finite element method* (PE-FEM) for the approximate solution of (5) or (6) defined on polytopal domains  $\Omega_h$  resulting from meshing of the domain  $\Omega$  by affine simplices. To achieve optimal accuracy even if  $\Omega$  has a curved boundary, we force the extension of the finite element solution to weakly match the given data on the curved boundary of the continuous problem.

We define the bilinear forms  $D_h(\cdot, \cdot) : H^1(\Omega_h) \times H^1(\Omega_h) \rightarrow \mathbb{R}$  and  $N_h(\cdot, \cdot) : H^1(\Omega_h) \times H^1(\Omega_h) \rightarrow \mathbb{R}$  as

$$(7) \quad \begin{aligned} D_h(u, v) &:= \int_{\Omega_h} \tilde{p} \nabla u \cdot \nabla v \, d\mathbf{x} \quad \forall u, v \in H^1(\Omega_h), \\ N_h(u, v) &:= \int_{\Omega_h} (\tilde{p} \nabla u \cdot \nabla v + \tilde{q} u v) \, d\mathbf{x} \quad \forall u, v \in H^1(\Omega_h), \end{aligned}$$

respectively.

For clarity, we first state the PE-FEM for the Dirichlet and Neumann problems in a form involving an analytic extension operator. Then we proceed to introduce versions of the methods, which use averaged Taylor polynomials to define the extensions, and are more amenable to rigorous analysis.

**The PE-FEM for the Dirichlet problem.** Seek  $u_h \in V_h^k$  such that

$$(8) \quad D_h(u_h, v) = \langle \tilde{f}, v \rangle_{\Omega_h} \quad \forall v \in V_{h,0}^k$$

---

<sup>2</sup>The existence of  $C^k$  extensions for the problem coefficients is a consequence of the Tietze-Urysohn extension theorem [10]. The existence of bounded extensions  $\tilde{f} \in H^{k-1}(\mathbb{R}^N)$  for  $k = 2, 3, \dots$  is a classical result of Sobolev spaces [1]. For  $k = 1$ , we can construct  $\tilde{f}$  by extending  $f$  to zero outside of  $\Omega$ . For  $k = 0$ , we can construct  $\tilde{f}_n$  as follows. Because  $L^2(\Omega)$  is dense in  $H^{-1}(\Omega)$ , we can write  $f$  as the limit of a sequence  $f_n \in L^2(\Omega)$ . We construct the functions  $\tilde{f}_n \in L^2(\mathbb{R}^N)$  by extending the functions  $f_n$  to zero outside of  $\Omega$ . We note that  $\tilde{f}_n$  is a Cauchy sequence in  $H^{-1}(\mathbb{R}^N)$  because  $\|\tilde{f}_n - \tilde{f}_m\|_{-1, \mathbb{R}^N} \leq \|f_n - f_m\|_{-1, \Omega}$  (recall that  $\|u\|_{-1, \Omega} := \sup_{v \in H^1(\Omega)} (u, v)_{\Omega} / \|v\|_{1, \Omega}$ ). Therefore  $\tilde{f}_n$  is convergent in  $H^{-1}(\mathbb{R}^N)$  and we define  $\tilde{f}$  to be its limit.

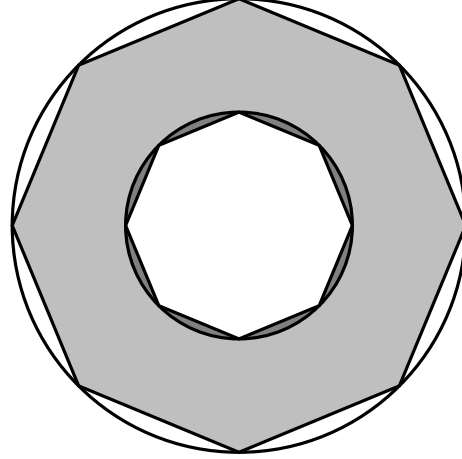


FIGURE 3. The area between the concentric circles is the given domain  $\Omega$ , and the area between the concentric octagons is the approximate domain  $\Omega_h$  (the regions covered by the two shades of gray). The light gray region is  $\Omega \cap \Omega_h$ . The dark gray regions are in  $\Omega_h$  but not in  $\Omega$  so extensions of functions defined on  $\Omega$  are needed in those regions.

and

$$(9) \quad \sum_i \langle E_{\mathcal{K}_{j_i}}(u_h) \circ \boldsymbol{\eta}(\boldsymbol{\xi}), \mu \rangle_{\mathcal{E}_i} = \langle g_D \circ \boldsymbol{\eta}(\boldsymbol{\xi}), \mu \rangle_{\Gamma_h} \quad \forall \mu \in W_h^k = V_h^k|_{\Gamma_h},$$

where  $E_{\mathcal{K}_{j_i}}(u_h)$  is the analytic extension operator that extends the polynomial  $u_h|_{\mathcal{K}_{j_i}}$  to a unique polynomial over  $\mathbb{R}^N$ . Implementation of this method requires the evaluation of  $E_{\mathcal{K}_{j_i}}(u_h) \circ \boldsymbol{\eta}(\boldsymbol{\xi})$  at a set of quadrature points  $\{\boldsymbol{\xi}_q\}$  on  $\mathcal{E}_i$ . This can be accomplished by evaluating the polynomial basis functions that generate  $u_h|_{\mathcal{K}_{j_i}}$  at the points  $\{\boldsymbol{\eta}(\boldsymbol{\xi}_q)\}$  that can be outside the element  $\mathcal{K}_{j_i}$ .

**The PE-FEM for the Neumann problem.** Seek  $u_h \in V_h^k$  such that

$$(10) \quad N_h(u_h, v) + \boldsymbol{\tau}_N(u_h, v) = \langle \tilde{f}, v \rangle_{\Omega_h} + \langle g_N \circ \boldsymbol{\eta}(\boldsymbol{\xi}), v \rangle_{\Gamma_h} \quad \forall v \in V_h^k,$$

where

$$(11) \quad \boldsymbol{\tau}_N(u_h, v) := \sum_i \left\langle \tilde{p} \circ \boldsymbol{\eta}(\boldsymbol{\xi}) \nabla (E_{\mathcal{K}_{j_i}}(u_h) \circ \boldsymbol{\eta}(\boldsymbol{\xi})) \cdot \mathbf{n} - \tilde{p} \nabla u_h \cdot \mathbf{n}_h, v \right\rangle_{\mathcal{E}_i}$$

is an auxillary term that provides additional accuracy to the standard finite element formulation. When  $\Gamma_h = \Gamma$  and  $\boldsymbol{\eta}$  is taken to be the identity operator, we have that  $\boldsymbol{\tau}_N(u_h, v) = 0$ .

Section 5 provides additional details about the implementation of the method.

In order to analyze the method, we reformulate the PE-FEM problem so that it is well-defined also for trial functions in  $H^k(\Omega_h)$ . In particular we need to generalize the extension operator  $E_{\mathcal{K}_{j_i}}$  to functions in Sobolev spaces. We achieve this by using averaged Taylor polynomials. The reformulated Dirichlet and Neumann PE-FEM problems will be equivalent to the ones in (8)–(11) whenever  $u_h \in V_h^k$ .

**3.1. Averaged Taylor polynomial extensions.** The mismatch between the exact domain  $\Omega$  and its polygonal approximation  $\Omega_h$  requires approximation of the boundary condition data on  $\Gamma_h$ . In this section, we focus on the extension of functions belonging to  $H^{k+1}(\Omega_h)$  from the approximate boundary  $\Gamma_h$  onto the true boundary  $\Gamma$ . A common approach is to approximate the true boundary condition data on  $\Gamma_h$  by a low-order reconstruction. However, due to the geometric error resulting from the approximation of the domain, this approach restricts the numerical solution to be at best second-order accurate regardless of the degree of the underlying finite element space. Here, instead of interpolating the boundary condition data, we *extend* the finite element solution from the approximate boundary  $\Gamma_h$  to the true boundary  $\Gamma$  and require it to weakly match the boundary condition data prescribed on that boundary. The main tool we use for defining this extension is the averaged Taylor polynomials, described below.

For every  $\mathcal{E}_i \in \Gamma_h$  let  $\{S^{i,\ell}\}$  denote a family, indexed by  $\ell$ , of disjoint star-shaped domains with respect to the balls  $\sigma^{i,\ell} \subset \mathcal{K}_{j_i} \cap \Omega$  such that  $S^{i,\ell} \cap \mathcal{K}_{j_{i'}} = \emptyset$  for  $i \neq i'$ ,  $\text{diam}(S^{i,\ell}) \leq C\delta_h$ , and  $\overline{\bigcup_{i,\ell} S^{i,\ell}} \supset \overline{\Omega_h \setminus (\Omega \cap \Omega_h)}$ . We also require that  $\overline{S^{i,\ell}} \cap \eta(\mathcal{E}_i) \subset S^{i,\ell}$  and  $\overline{S^{i,\ell}} \cap \mathcal{E}_i \subset S^{i,\ell}$  and that  $\sup_{i,\ell} \frac{\text{diam}(S^{i,\ell})}{\text{radius}(\sigma^{i,\ell})} \leq C$  with  $C$  independent of  $\delta_h$ . See Figure 4 for an illustration of how star-shaped domains  $S^{i,\ell}$  can be constructed for triangular meshes.

*Remark 1.* Whereas it is possible to construct the star-shaped domains  $S^{i,\ell}$  with the properties listed above for simple geometries/meshes, we do not have a proof for general domains and shape-regular meshes considered in this paper. If we allow the domains  $S^{i,\ell}$  to overlap up to a finite number of times, it may be possible to follow the construction in [26, Section 2.2]. However, this would further increase the complexity of the analysis so we prefer to limit our analysis to the case for which the domains  $S^{i,\ell}$  do not overlap.

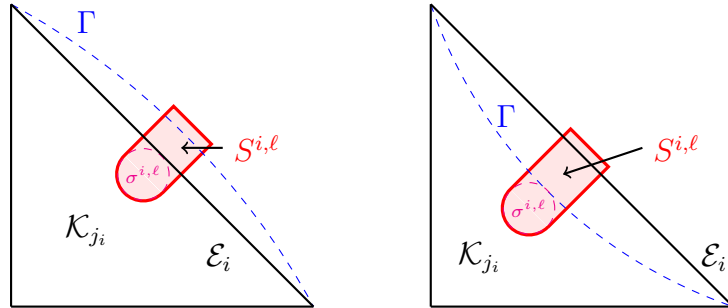


FIGURE 4. Illustration of the construction of a star-shaped (with respect to  $\sigma^{i,\ell}$ ) set  $S^{i,\ell} \subset \mathbb{R}^N$  for  $\Gamma \cap \mathcal{K}_{j_i} = \emptyset$  (left) and  $\Gamma \cap \mathcal{K}_{j_i} \neq \emptyset$  (right).

Following [5], we define, for  $\mathbf{x} \in \mathbb{R}^N$  and  $v \in L^2(\Omega \cap \Omega_h)$ , the averaged Taylor polynomial<sup>3</sup>

$$(12) \quad T_h^k(v)|_{\mathbf{x}} := \sum_{i,\ell} \mathbf{1}_{S^{i,\ell}}(\mathbf{x}) \int_{\sigma^{i,\ell}} \left( \sum_{|\boldsymbol{\alpha}|=0}^k \frac{1}{\boldsymbol{\alpha}!} D^{\boldsymbol{\alpha}} v(\mathbf{y})(\mathbf{x} - \mathbf{y})^{\boldsymbol{\alpha}} \phi_{\ell}(\mathbf{y}) \right) d\mathbf{y},$$

where  $\phi_{\ell}(\mathbf{y})$  is a cutoff function and  $\mathbf{1}_{S^{i,\ell}}(\mathbf{x})$  denotes the indicator function for the set  $S^{i,\ell}$ , i.e.,  $\mathbf{1}_{S^{i,\ell}}(\mathbf{x}) = 1$  if  $\mathbf{x} \in S^{i,\ell}$  and vanishes otherwise. Note that  $T_h^k$  is meaningful only for  $\mathbf{x} \in \bigcup_{i,\ell} S^{i,\ell}$  and is zero otherwise. For any  $\boldsymbol{\xi} \in \Gamma_h$  and its image  $\boldsymbol{\eta}(\boldsymbol{\xi}) \in \Gamma$  and for  $v \in L^2(\overline{\Omega})$ , we write

$$(13) \quad v \circ \boldsymbol{\eta}(\boldsymbol{\xi}) = T_h^k(v)|_{\boldsymbol{\eta}(\boldsymbol{\xi})} + R_h^k(v)|_{\boldsymbol{\eta}(\boldsymbol{\xi})}.$$

For  $v \in H^{k+1}(\mathbb{R}^N)$  we have  $\|R_h^k(v)|_{\boldsymbol{\eta}(\boldsymbol{\xi})}\|_{0,\Gamma_h} \leq C \delta_h^{k+\frac{1}{2}} |v|_{k+1,\mathbb{R}^N}$ ; see Lemma 2. If  $v \in \overline{V}_h^k$ , then in every  $\mathcal{K}_{j_i}$ ,  $v$  is a polynomial of degree  $k$  and therefore  $T_h^k(v)$  exactly reproduces  $v$  in any  $\mathcal{K}_{j_i}$  adjacent to the boundary and is equivalent to the classical Taylor polynomial. For  $v \in \overline{V}_h^k$  we can therefore write, for a generic  $\mathbf{y}_i \in \mathcal{K}_{j_i}$ ,

$$\begin{aligned} T_h^k(v)|_{\mathbf{x}} &= \sum_{i,\ell} \mathbf{1}_{S^{i,\ell}}(\mathbf{x}) \sum_{|\boldsymbol{\alpha}|=0}^k \frac{1}{\boldsymbol{\alpha}!} D^{\boldsymbol{\alpha}} v(\mathbf{y}_i) (\mathbf{x}_i - \mathbf{y}_i)^{\boldsymbol{\alpha}} \\ &= \sum_i \mathbf{1}_{(\bigcup_j S^{i,\ell})}(\mathbf{x}) \sum_{|\boldsymbol{\alpha}|=0}^k \frac{1}{\boldsymbol{\alpha}!} D^{\boldsymbol{\alpha}} v(\mathbf{y}_i) (\mathbf{x}_i - \mathbf{y}_i)^{\boldsymbol{\alpha}}. \end{aligned}$$

Setting  $\mathbf{y}_i = \boldsymbol{\xi} \in \mathcal{E}_i$  and  $\mathbf{x} = \boldsymbol{\eta}(\boldsymbol{\xi})$  we now have that

$$(14) \quad T_h^k(v)|_{\boldsymbol{\eta}(\boldsymbol{\xi})} = \sum_{|\boldsymbol{\alpha}|=0}^k \frac{1}{\boldsymbol{\alpha}!} D_h^{\boldsymbol{\alpha}} v(\boldsymbol{\xi}) (\boldsymbol{\eta}(\boldsymbol{\xi}) - \boldsymbol{\xi})^{\boldsymbol{\alpha}}$$

which is well-defined for any  $\boldsymbol{\xi} \in \Gamma_h$  and  $v \in \overline{V}_h^k$ . Note that if  $\boldsymbol{\xi} \in \mathcal{E}_i$  and  $v$  is a polynomial of degree  $k$  defined on  $\mathcal{K}_{j_i}$  then  $T_h^k(v)|_{\boldsymbol{\eta}(\boldsymbol{\xi})} \equiv E_{\mathcal{K}_{j_i}}(v) \circ \boldsymbol{\eta}(\boldsymbol{\xi})$ . For convenience, we also define  $T_h^{k',k}$  as

$$(15) \quad T_h^{k',k}(v)|_{\boldsymbol{\eta}(\boldsymbol{\xi})} = \sum_{|\boldsymbol{\alpha}|=k'}^k \frac{1}{\boldsymbol{\alpha}!} D_h^{\boldsymbol{\alpha}} v(\boldsymbol{\xi}) (\boldsymbol{\eta}(\boldsymbol{\xi}) - \boldsymbol{\xi})^{\boldsymbol{\alpha}}.$$

Clearly  $T_h^k = T_h^{0,k}$ . For vector functions  $\mathbf{v}$ , we introduce the vector operator  $\mathbf{T}_h^k(\mathbf{v}) = (T_h^k v_n)_{n=1}^N$ . We use this notation in particular for gradients of scalar functions, i.e.,  $\mathbf{T}_h^k(\nabla v)$ .

**3.2. PE-FEMs using averaged Taylor polynomials.** Using the averaged Taylor polynomial extensions and Taylor's theorem allows one to represent the Dirichlet and Neumann data prescribed at  $\boldsymbol{\eta}(\boldsymbol{\xi}) \in \Gamma$  as functions of  $\boldsymbol{\xi} \in \Gamma_h$  given by

$$(16) \quad g_D \circ \boldsymbol{\eta}(\boldsymbol{\xi}) = T_h^k(\tilde{u})|_{\boldsymbol{\eta}(\boldsymbol{\xi})} + R_h^k(\tilde{u})|_{\boldsymbol{\eta}(\boldsymbol{\xi})}$$

and

$$(17) \quad g_N \circ \boldsymbol{\eta}(\boldsymbol{\xi}) = \tilde{p} \circ \boldsymbol{\eta}(\boldsymbol{\xi}) \left( \mathbf{T}_h^{k-1}(\nabla \tilde{u})|_{\boldsymbol{\eta}(\boldsymbol{\xi})} \cdot \mathbf{n} + \mathbf{R}_h^{k-1}(\nabla \tilde{u})|_{\boldsymbol{\eta}(\boldsymbol{\xi})} \cdot \mathbf{n} \right),$$

---

<sup>3</sup>Averaged Taylor polynomials on star-shaped domains  $S^{i,\ell}$  are defined for functions in  $L^1(\sigma^{i,\ell})$ ; see [5, Corollary 4.1.15].

respectively, where  $R_h^k(\tilde{u})|_{\boldsymbol{\eta}(\xi)}$  and  $\mathbf{R}_h^{k-1}(\nabla \tilde{u})|_{\boldsymbol{\eta}(\xi)}$  denote the remainder terms of the averaged Taylor polynomials. These representations are used in the definition of the boundary conditions for the PE-FEM formulations.

**The PE-FEM Dirichlet problem.** We use (16) to supply the Dirichlet boundary condition (9) for the problem posed on the approximate domain  $\Omega_h$ . Note that for  $u_h \in V_h^k$ , the remainder term in (16) vanishes. Then, for the Taylor polynomial extension approach, the *PE-FEM Dirichlet problem* (8) and (9) is to seek  $u_h \in V_h^k$  such that

$$(18) \quad \begin{cases} D_h(u_h, v) = \langle \tilde{f}, v \rangle_{\Omega_h} & \forall v \in V_{h,0}^k, \\ \langle T_h^k u_h(\boldsymbol{\xi})|_{\boldsymbol{\eta}(\boldsymbol{\xi})}, \mu \rangle_{\Gamma_h} = \langle g_D \circ \boldsymbol{\eta}(\boldsymbol{\xi}), \mu \rangle_{\Gamma_h} & \forall \mu \in W_h^k = V_h^k|_{\Gamma_h}. \end{cases}$$

*Remark 2.* The problem (18) is not a Dirichlet problem, per se. The boundary condition, i.e., the second equation in (18), involves derivatives of the unknown  $u_h$  of order up to  $k$  evaluated along the boundary edges  $\mathcal{E}_i$  of the approximate domain  $\Gamma_h$ . The inclusion of these derivatives in the boundary condition imposed on the approximate boundary  $\Gamma_h$  is, of course, what leads to the optimal accuracy of the PE-FEM approximation.

In order to use the same space for the trial and test functions, we reformulate the problem (18) as follows. Let  $(\cdot)_\star : V_h^k \rightarrow W_h^k$  denote the trace operator and  $\mathcal{R}_h : W_h^k \rightarrow V_h^k$  a discrete linear lifting operator. Also, let

$$(19) \quad B_{h,D}^\theta(u, v) := D_h(u, v - \mathcal{R}_h v_\star) + \theta_h \langle T_h^k u(\boldsymbol{\xi})|_{\boldsymbol{\eta}(\boldsymbol{\xi})}, v \rangle_{\Gamma_h}$$

and

$$(20) \quad F_{h,D}^\theta(v) := \langle \tilde{f}, v - \mathcal{R}_h v_\star \rangle_{\Omega_h} + \theta_h \langle g_D \circ \boldsymbol{\eta}(\boldsymbol{\xi}), v \rangle_{\Gamma_h}.$$

We then seek  $u_h \in V_h^k$  such that

$$(21) \quad B_{h,D}^\theta(u_h, v) = F_{h,D}^\theta(v) \quad \forall v \in V_h^k.$$

Because  $v - \mathcal{R}_h v_\star$  spans the entirety of  $V_{h,0}^k$ , the formulations (18) and (21) are equivalent for any nonzero  $\theta_h \in \mathbb{R}$ . The choice of scaling factor  $\theta_h$  does not affect the solution, but choosing  $\theta_h \sim O(h^{-1})$  balances, with respect to  $h$ , the two terms on the right-hand side of (19), is needed to prove the coercivity of the bilinear form  $B_{h,D}^\theta$ , and may positively affect properties of the stiffness matrix; see §4.1.

A careful inspection shows that the problems (21), (18), and (8) are equivalent.

**The PE-FEM Neumann problem.** The Taylor series representation (17) of the Neumann data implies that

$$(22) \quad 0 \approx g_N \circ \boldsymbol{\eta}(\boldsymbol{\xi}) - \tilde{p} \circ \boldsymbol{\eta}(\boldsymbol{\xi}) \cdot \mathbf{T}_h^{k-1}(\nabla u_h)|_{\boldsymbol{\eta}(\boldsymbol{\xi})} \cdot \mathbf{n}.$$

By adding  $\tilde{p}(\boldsymbol{\xi}) \nabla u_h \cdot \mathbf{n}_h$  to both sides, we can approximate the Neumann data as

$$(23) \quad \tilde{p}(\boldsymbol{\xi}) \nabla u_h \cdot \mathbf{n}_h \approx g_N \circ \boldsymbol{\eta}(\boldsymbol{\xi}) + \tilde{p}(\boldsymbol{\xi}) \nabla u_h \cdot \mathbf{n}_h - \tilde{p} \circ \boldsymbol{\eta}(\boldsymbol{\xi}) \cdot \mathbf{T}_h^{k-1}(\nabla u_h)|_{\boldsymbol{\eta}(\boldsymbol{\xi})} \cdot \mathbf{n}.$$

The discrete weak form (10) and (11) of (4) is given by

$$N_h(u_h, v) - \langle \tilde{p}(\boldsymbol{\xi}) \nabla u_h \cdot \mathbf{n}_h, v \rangle_{\Gamma_h} = \langle \tilde{f}, v \rangle_{\Omega_h} \quad \forall v \in V_h^k.$$

Incorporating (23) yields the *PE-FEM Neumann formulation*: seek  $u_h \in V_h^k$  such that

$$(24) \quad B_{h,N}(u_h, v) = F_{h,N}(v) \quad \forall v \in V_h^k,$$

where

$$(25) \quad B_{h,N}(u_h, v) := N_h(u_h, v) + \tau_N(u_h, v)$$

with

$$\tau_N(u_h, v) := \langle \tilde{p} \circ \boldsymbol{\eta}(\boldsymbol{\xi}) \mathbf{T}_h^{k-1}(\nabla u_h) \Big|_{\boldsymbol{\eta}(\boldsymbol{\xi})} \cdot \mathbf{n} - \tilde{p}(\boldsymbol{\xi}) \nabla u_h \cdot \mathbf{n}_h, v \rangle_{\Gamma_h}$$

and

$$(26) \quad F_{h,N}(v) := \langle \tilde{f}, v \rangle_{\Omega_h} + \langle g_N \circ \boldsymbol{\eta}(\boldsymbol{\xi}), v \rangle_{\Gamma_h} \quad \forall v \in V_h^k.$$

A careful inspection shows that the problems (24) and (10) are equivalent.

*Remark 3.* There is a price to pay for obtaining optimal convergence rates for higher-order finite element methods on polygonal domains for problems posed on nonpolygonal domains, namely that the discretized systems (18) and (24) are not symmetric, even for given symmetric problems, i.e., even if  $D_h(\cdot, \cdot)$  and  $N_h(\cdot, \cdot)$  are symmetric bilinear forms. However, if these forms are indeed symmetric and if an iterative linear system solver is used, the additional computational cost due to any destruction of symmetry is not so burdensome. The contributions to the stiffness matrices associated with those forms, being associated with interior nodes of the mesh, are much larger than the contributions associated with the terms causing the lack of symmetry because the latter are associated with boundary nodes.

#### 4. ANALYSIS OF THE PE-FEM FORMULATIONS

We now show that (21) and (24) are well-posed and satisfy a *polynomial preserving property*. Then, we prove that the PE-FEM formulations for  $k$ th order Lagrangian finite element spaces are optimally accurate in the  $H^1(\Omega_h)$ -norm. Additionally, we prove optimal  $L^2(\Omega_h)$  convergence for the PE-FEM Dirichlet formulation under certain conditions on  $\Omega_h$  and additional regularity on  $u$ . Throughout the section we assume that  $\Omega_h$  consists of a regular mesh [9] and let  $\underline{p} := \min_{x \in \Omega_h} \tilde{p}(x)$ ,  $\bar{p} := \max_{x \in \Omega_h} \tilde{p}(x)$ , and  $\underline{q} = \min_{x \in \Omega_h} \tilde{q}(x)$ .

##### 4.1. Well-posedness of the PE-FEMs.

**Theorem 1** (Well-posedness of the PE-FEM Dirichlet approximation). *Let  $B_{h,D}^\theta(\cdot, \cdot)$  be defined as in (19) with  $\underline{p} > 0$ . Assume that  $\theta_h \geq C_\theta h^{-1}$  with  $C_\theta$  large enough and assume that  $\delta_h \sim o(h^{\frac{3}{2}})$ . Then, for  $h$  small enough and  $k = 1, 2, \dots$ , we have that*

$$(27) \quad B_{h,D}^\theta(u, v) \leq C \left( \bar{p} + \theta_h \left( 1 + \sum_{|\alpha|=1}^k h^{\frac{1}{2}-|\alpha|} \delta_h^{|\alpha|} \right) \right) \|u\|_{1,\Omega_h} \|v\|_{1,\Omega_h} \quad \forall u, v \in V_h^k$$

and

$$(28) \quad B_{h,D}^\theta(u, u) \geq \gamma_D \|u\|_{1,\Omega_h}^2 \quad \forall u \in V_h^k.$$

If  $g_D \circ \boldsymbol{\eta}(\boldsymbol{\xi}) \in H^{1/2}(\Gamma_h)$ , then (21) has a unique solution  $u_h$  and that solution satisfies the stability bound

$$(29) \quad \|u_h\|_{1,\Omega_h} \leq C (\|\tilde{f}\|_{-1,\Omega_h} + \|g_D \circ \boldsymbol{\eta}(\boldsymbol{\xi})\|_{1/2,\Gamma_h}).$$

The proof is provided in §D.1.

**Theorem 2** (Well-posedness of the PE-FEM Neumann approximation). *Let  $B_{h,N}(u, v)$  be defined as in (25). Assume that  $\delta_h \sim o(h^{\frac{3}{2}})$ ,  $\tilde{p}, \tilde{q} > 0$  in  $\Omega_h$ , and  $\tilde{p} > 0$  on  $\Gamma$ . Then, for  $h$  small enough and  $k = 1, 2, \dots$ , we have that*

$$(30) \quad B_{h,N}(u, v) \leq C \|u\|_{1,\Omega_h} \|v\|_{1,\Omega_h} \quad \forall u, v \in V_h^k$$

and

$$(31) \quad B_{h,N}(u, u) \geq \gamma_N \|u\|_{\Omega_h}^2 \quad \forall u \in V_h^k.$$

If  $g_N \circ \boldsymbol{\eta}(\xi) \in H^{-1/2}(\Gamma_h)$ , then (24) has a unique solution  $u_h$  and that solution satisfies the stability bound

$$(32) \quad \|u_h\|_{1,\Omega_h} \leq C \gamma_N^{-1} (\|\tilde{f}\|_{-1,\Omega_h} + \|g_N \circ \boldsymbol{\eta}(\xi)\|_{-1/2,\Gamma_h}).$$

Finally, for all  $u, v \in H^1(\Omega_h)$  such that  $u|_{\mathcal{K}_n} \in H^{k+1}(\mathcal{K}_n)$  for all  $\mathcal{K}_n \subset \Omega_h$ , we have that, for  $k = 2, 3, \dots$ ,

$$(33) \quad \begin{aligned} B_{h,N}(u, v) \leq C & \left[ \|u\|_{1,\Omega_h} + (\delta_h h^{\frac{3}{2}} + h^{\frac{5}{2}}) \|u\|_{3,\Omega_h} \right. \\ & \left. + \delta_h^{\frac{1}{2}} \|u\|_{2,\Omega_h} + \delta_h^{k-\frac{1}{2}} \|u\|_{k+1,\Omega_h} \right] \|v\|_{1,\Omega_h}. \end{aligned}$$

The proof is provided in §D.2.

*Remark 4.* Theorems 1 and 2 establish well-posedness of the PE-FEM Dirichlet and Neumann problems for the linear diffusion-reaction equation. We remark that if a convection operator also appears along with the elliptic operator, the above analysis remains, for the most part, unchanged, i.e., it can be treated in the same manner as convection terms are handled by standard finite element methods.

*Remark 5.* Bounds (29) and (32) imply that the solution of the PE-FEM remains stable as  $h \rightarrow 0$ .

**4.2. Polynomial preserving property.** The finite element space  $V_h^k$  contains the *global* polynomial space  $P_k(\Omega_h)$ . Thus, exact recovery of global polynomial fields in  $P_k(\Omega_h)$  is a desirable property for a finite element method implemented using this space. While such a “patch test” is not sufficient for optimal convergence, it provides a useful diagnostic tool for code verification.

It is straightforward to show that the PE-FEM preserves global polynomial fields. Given an  $r \in P_k(\Omega_h)$  and a forcing function  $\tilde{f} = Lr$ , where  $L$  denotes, as appropriate, either the strong operator in (3) for Dirichlet problems or the strong operator in (4) for Neumann problems, it is clear that  $r$  satisfies

$$D_h(r, v) = \langle \tilde{f}, v \rangle_{\Omega_h} \quad \forall v \in V_{h,0}^k \quad \text{and} \quad N_h(r, v) = \langle \tilde{f}, v \rangle_{\Omega_h} \quad \forall v \in V_h^k.$$

Because Taylor series preserve polynomials, the boundary conditions of (21) and (24) are satisfied by  $r$  if  $g_D = r|_\Gamma$  and  $g_N = (\tilde{p} \nabla r \cdot \mathbf{n})|_\Gamma$ . Furthermore, if the conditions in Theorems 1 and 2 hold,  $u_h = r$  is the unique solution of the PE-FEM equations. Thus, we have established the following proposition.

**Proposition 1.** *The PE-FEMs (cf. (21) and (24)) are polynomial preserving.*

**4.3. Error estimates for PE-FEM approximations.** Using results from §4.1, we now prove optimal  $H^1(\Omega_h)$ -norm error estimates for the Dirichlet and Neumann PE-FEM problems and optimal  $L^2(\Omega_h)$ -norm error estimates for the Dirichlet PE-FEM problem.

**Theorem 3** ( $H^1(\Omega_h)$ -norm error estimate for the Dirichlet PE-FEM approximation). *Assume that  $f \in H^{k-1}(\Omega)$ ,  $g_D \in H^{k+\frac{1}{2}}(\Gamma)$ , and the hypotheses of Theorem 1 hold with the additional assumption that  $\delta_h \sim o(h^{\frac{3}{2}})$  if  $d = 2$  and  $\delta_h \sim O(h^2)$  if  $d = 3$ . Let  $u_h \in V_h^k$  denote the solution of (21),  $u \in H^{k+1}(\Omega)$  the solution to (5), and  $\tilde{u} \in H^{k+1}(\mathbb{R}^N)$  the extension of the latter. Then,*

$$\|\tilde{u} - u_h\|_{1,\Omega_h} \leq Ch^k(\|u\|_{k+1,\Omega} + \|f\|_{k-1,\Omega}) \quad \text{for } k = 2, 3, \dots$$

The proof is given in §E.1.

**Theorem 4** ( $L^2(\Omega_h)$ -norm error estimate for the Dirichlet PE-FEM approximation). *Assume that  $\delta_h \sim O(h^2)$ ,  $f \in H^k(\Omega)$ , and the hypotheses of Theorem 1 hold. Let  $u_h \in V_h^k$  denote the solution of (21),  $u \in H^{k+\frac{3}{2}}(\Omega)$  the solution to (5), and  $\tilde{u} \in H^{k+\frac{3}{2}}(\mathbb{R}^N)$  the extension of the latter. Then,*

$$(34) \quad \|\tilde{u} - u_h\|_{0,\Omega_h} \leq Ch^{k+s}(\|u\|_{k+1,\Omega} + |\tilde{u}|_{k+1,\Gamma_h} + \|f\|_{k,\Omega}) \quad \text{for } k = 2, 3, \dots,$$

where  $s \in (\frac{1}{2}, 1]$  is a constant dependent on the largest interior angle of  $\partial\Omega_h$ , given  $h$  is small enough. Additionally, if  $\partial\Omega_h$  is a convex polytope, we have that (34) holds with  $s = 1$ .

The proof is given in §E.2.

**Theorem 5** ( $H^1(\Omega_h)$ -norm error estimate for the Neumann PE-FEM approximation). *Assume that  $f \in H^{k-1}(\Omega)$ ,  $g_N \in H^{k-\frac{1}{2}}(\Gamma_h)$ , and the hypotheses of Theorem 2 hold. Let  $u_h \in V_h^k$  denote the solution of (24),  $u \in H^{k+1}(\Omega)$  the solution to (6), and  $\tilde{u} \in H^{k+1}(\mathbb{R}^N)$  the extension of the latter. Then, if  $\delta_h \sim O(h^2)$ , we have the bound*

$$\|\tilde{u} - u_h\|_{1,\Omega_h} \leq Ch^k(\|\tilde{u}\|_{k+1} + \|f\|_{k-1,\Omega}) \quad \text{for } k = 2, 3, \dots$$

The proof is given in §E.3.

*Remark 6.* Although our results do not include optimal  $L^2$ -norm error estimates for the Neumann problem, numerical results given in §6 suggest that the PE-FEM formulation is optimally accurate in this case as well.

## 5. IMPLEMENTATION

The conversion of any finite element code into a PE-FEM code is a relatively simple matter as it only requires coding the additional terms in (9) and (11) which are relatively minor variations of the standard assembly process on each element.

**5.1. The mapping  $\eta(\xi)$ .** Whereas different choices of mappings  $\eta : \Gamma_h \rightarrow \Gamma$  are possible, in our numerical experiments we use the mapping

$$(35) \quad \eta(\xi) := \arg \min_{\mathbf{x} \in \Gamma} |\mathbf{x} - \xi|$$

that guarantees that  $|\eta(\xi) - \xi| = O(h^2)$ . In the implementation, we apply the mapping to  $\xi$  belonging to the set of nodes or quadrature points lying on  $\Gamma_h$ .

**5.2. Implementation of the PE-FEM Dirichlet problem.** In (9), the essential boundary condition is imposed on the piecewise polynomial extensions in a weak, variational, sense. In order to compute the boundary integrals using quadrature rules, one can compute the term  $(E_{\mathcal{K}_{j_i}}(u_h) \circ \boldsymbol{\eta}(\boldsymbol{\xi}_q))$  at quadrature points  $\boldsymbol{\xi}_q \in \mathcal{E}_i$  by evaluating the polynomial basis functions that generate  $u_h|_{\mathcal{K}_{j_i}}$  at  $\boldsymbol{\eta}(\boldsymbol{\xi}_q)$ .

Alternatively, for two-dimensional Type A meshes, it is possible to prescribe the Dirichlet condition in a strong sense:

$$E_{\mathcal{K}_{j_i}}(u_h) \circ \boldsymbol{\eta}(\boldsymbol{\xi}_i) = g_D \circ \boldsymbol{\eta}(\boldsymbol{\xi}_i)$$

for all nodes  $\boldsymbol{\xi}_i \in \Gamma_h$  associated with the degrees of freedom of  $W_h^k$ . Here,  $\mathcal{K}_{j_i}$  denotes the element whose closure contains  $\boldsymbol{\xi}_i$ . The element  $\mathcal{K}_{j_i}$  is not uniquely defined if  $\boldsymbol{\xi}_i$  is a vertex of the triangulation. However, in this case, for two-dimensional Type A meshes we have that  $\boldsymbol{\xi}_i \in \Gamma \cap \Gamma_h$  and therefore the extension operators reduce to the identity operator.

**5.3. Implementation of the PE-FEM Neumann problem.** The PE-FEM Neumann problem can be obtained by adding the term (11),

$$\sum_i \left\langle \tilde{p} \circ \boldsymbol{\eta}(\boldsymbol{\xi}) \nabla (E_{\mathcal{K}_{j_i}}(u_h) \circ \boldsymbol{\eta}(\boldsymbol{\xi})) \cdot \mathbf{n} - \tilde{p} \nabla u_h \cdot \mathbf{n}_h, v \right\rangle_{\mathcal{E}_i},$$

to a standard finite element code, and by evaluating the Neumann data  $g_N$  at the points on the true boundary  $\Gamma$  using the mapping  $\boldsymbol{\eta}$ . In particular, when computing the integrals using quadrature rules, one can compute the term  $\nabla (E_{\mathcal{K}_{j_i}}(u_h) \circ \boldsymbol{\eta}(\boldsymbol{\xi}_q))$  at quadrature points by evaluating the gradient of the polynomial basis functions that generates  $u_h|_{\mathcal{K}_{j_i}}$  at  $\boldsymbol{\eta}(\boldsymbol{\xi}_q)$  and can compute the right-hand side by evaluating  $g_N$  at  $\boldsymbol{\eta}(\boldsymbol{\xi}_q)$ . The outer unit normal vectors  $\mathbf{n}_h$  at  $\boldsymbol{\xi}_q$  and  $\mathbf{n}$  at  $\boldsymbol{\eta}(\boldsymbol{\xi}_q)$  need to be computed as well.

**5.4. Computation of  $\tilde{p}(x), \tilde{q}(x)$ , and  $\tilde{f}$ .** The formal statement of the PE-FEM in (18) and (24) requires extensions of  $p(x)$ ,  $q(x)$ , and the forcing data  $f$  into  $\mathbb{R}^N$ . Although possible in theory, such an extension is computationally impractical. Fortunately, the values of  $\tilde{p}(x)$ ,  $\tilde{q}(x)$ , and  $\tilde{f}(x)$  are only needed at a finite number of quadrature points in  $\Omega_h$ . This reduces the problem to one of accurate representation of the extended data at a finite number of quadrature points in  $\Omega_h$ . This problem is not exclusive to the PE-FEM and appears in most geometrically nonconforming methods (e.g. standard finite elements on polytopal approximations of nonconvex curved domains), not just the PE-FEM. For completeness, we describe a simple approach to obtain the necessary point values.

Specifically, given an  $O(h)$  neighborhood of a problematic quadrature point, one can generate the necessary values at this point by using a  $k$ th order polynomial least-squares fit of  $p$ ,  $q$ , and  $f$  in this neighborhood. Assuming that  $p, q, f \in W_\infty^{k+1}(\Omega)$  one should be able to show that this approach will yield optimal convergence rates along the same lines as in [28, Theorem 1.6]. We refer to [29] for additional details of least-squares recovery procedures from finite element data. We note that using such procedures introduces yet another variational crime into the formulation. However, analysis of such a crime is beyond the scope of this paper.

## 6. NUMERICAL EXAMPLES

In this section, we present illustrative numerical results for the Dirichlet and Neumann PE-FEM for both a convex and a nonconvex domain with circular boundaries. Additionally, we provide results for both boundary value problems on a flower-shaped domain with a significant boundary curvature.

**6.1. Convex domain.** The convex domain  $\Omega$  considered is the unit circle centered at  $(0,0)$  having radius 1. The coefficients are given by  $p(x,y) = q(x,y) = 1$  and the right-hand side  $f$  and the relevant boundary data are determined by inserting the exact solution  $u(x,y) = \cos(x)\cos(y)$  into the governing equations. A representative PE-FEM approximate solution is plotted in Figure 5 (left). We report on the convergence history for the PE-FEM in Table 2. We observe that optimal  $H^1(\Omega_h)$  and  $L^2(\Omega_h)$  convergence rates are achieved in all cases.

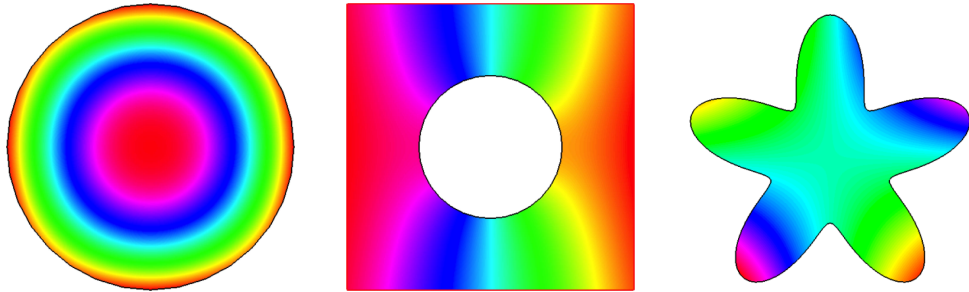


FIGURE 5. Numerical solutions computed by the PE-FEM. Left: solution of the circular domain problem computed using the Neumann PE-FEM with cubic elements. Center: solution for the nonconvex domain computed using the Dirichlet PE-FEM with cubic elements. Right: solution of the flower-shaped domain problem computed using the Neumann PE-FEM with cubic elements.

**6.2. Nonconvex domain.** We consider a nonconvex domain  $\Omega$  obtained by cutting a circular hole of radius  $\frac{1}{4}$ , centered at  $(0,0)$ , from the unit square  $[-0.5, 0.5]^2$ . The coefficients are given by  $p(x,y) = q(x,y) = 1$  and the necessary right-hand side  $f$  and boundary data are again determined by inserting the exact solution  $u(x,y) = -\frac{17}{16} \frac{x}{x^2+y^2}$  into the governing equations. We use the resulting Dirichlet boundary conditions on the outer boundary of the square because no special treatment is required to apply these conditions along straight edges. The PE-FEM conditions are utilized on the interior circular boundary. A representative PE-FEM approximate solution is plotted in Figure 5 (center). The convergence history for this example is summarized in Table 3. We again observe that optimal  $H^1(\Omega_h)$  and  $L^2(\Omega_h)$  convergence rates are achieved in all cases.

**6.3. Flower-shaped domain.** The domain  $\Omega$  considered in this numerical experiment has a boundary generated by the parametrization

$$\begin{bmatrix} x(\theta) \\ y(\theta) \end{bmatrix} = \begin{bmatrix} [0.5 + 0.2 \sin(5\theta)] \cos(\theta) \\ [0.5 + 0.2 \sin(5\theta)] \sin(\theta) \end{bmatrix} \quad \text{for } \theta \in (0, 2\pi].$$

TABLE 2. Convergence histories for the PE-FEM Dirichlet and Neumann PE-FEM approximations for the convex domain example. Optimal convergence rates are achieved with respect to both the  $L^2(\Omega_h)$ - and  $H^1(\Omega_h)$ -norms.

Quadratic elements ( $k = 2$ )				
$h$	Dirichlet		Neumann	
	$\ u - u_h\ _{0,\Omega_h}$	$\ u - u_h\ _{1,\Omega_h}$	$\ u - u_h\ _{0,\Omega_h}$	$\ u - u_h\ _{1,\Omega_h}$
0.583095	6.83996e-04	1.20924e-02	8.71677e-03	1.18623e-02
0.315543	8.71107e-05	2.96301e-03	1.29589e-03	2.93169e-03
0.165152	1.07759e-05	7.21901e-04	1.55799e-04	7.11529e-04
0.080322	1.28123e-06	1.81096e-04	1.99808e-05	1.79352e-04
0.045221	1.59731e-07	4.41786e-05	2.22425e-06	4.39835e-05
Rate	3.2283	2.1605	3.1932	2.1558
Cubic elements ( $k = 3$ )				
$h$	Dirichlet		Neumann	
	$\ u - u_h\ _{0,\Omega_h}$	$\ u - u_h\ _{1,\Omega_h}$	$\ u - u_h\ _{0,\Omega_h}$	$\ u - u_h\ _{1,\Omega_h}$
0.583095	3.11001e-05	7.19118e-04	2.74664e-04	7.11022e-04
0.315543	1.67332e-06	7.63497e-05	1.96586e-05	7.61091e-05
0.165152	1.06597e-07	1.00175e-05	9.82364e-07	9.95999e-06
0.080322	6.87903e-09	1.34472e-06	6.63858e-08	1.34119e-06
0.045221	4.33984e-10	1.66115e-07	2.73366e-09	1.65852e-07
Rate	4.2922	3.2024	4.4254	3.1993
Quartic elements ( $k = 4$ )				
$h$	Dirichlet		Neumann	
	$\ u - u_h\ _{0,\Omega_h}$	$\ u - u_h\ _{1,\Omega_h}$	$\ u - u_h\ _{0,\Omega_h}$	$\ u - u_h\ _{1,\Omega_h}$
0.583095	6.02698e-07	2.36345e-05	3.0114e-05	2.57857e-05
0.315543	2.24273e-08	1.41265e-06	1.72058e-06	1.59270e-06
0.165152	6.36060e-10	8.36391e-08	4.75739e-08	8.54912e-08
0.080322	1.73323e-11	5.12435e-09	1.41032e-09	5.11654e-09
Rate	5.2938	4.2606	5.0798	4.3162

The coefficients of the governing equation are again given by  $p(x, y) = q(x, y) = 1$  and the right-hand side  $f$  corresponds to the manufactured solution  $u(x, y) = e^{xy}$ . A stable numerical solution of this problem requires finer mesh, most likely due to the significant curvature of the boundary. A typical PE-FEM approximate solution is plotted in Figure 5 (right), while the PE-FEM convergence history for this example is summarized in Table 4. In all cases we observe optimal  $H^1(\Omega_h)$  and  $L^2(\Omega_h)$  convergence rates.

## 7. CONCLUDING REMARKS

This paper formulates and analyzes a new finite element method for second-order elliptic boundary value problems that remains optimally accurate when a computational domain  $\Omega$ , having a smooth curved boundary, is approximated by a polytope  $\Omega_h$ . We achieve optimal convergence rates by using polynomial extensions from the boundary of  $\Omega_h$  to the boundary of  $\Omega$  to impose weakly the boundary conditions.

TABLE 3. Convergence histories for PE-FEM Dirichlet and Neumann PE-FEM approximations for the nonconvex domain example. Optimal convergence rates are achieved with respect to both the  $L^2(\Omega_h)$ - and  $H^1(\Omega_h)$ -norms.

Quadratic elements ( $k = 2$ )				
$h$	Dirichlet		Neumann	
	$\ u - u_h\ _{0,\Omega_h}$	$\ u - u_h\ _{1,\Omega_h}$	$\ u - u_h\ _{0,\Omega_h}$	$\ u - u_h\ _{1,\Omega_h}$
0.353553	6.39714e-03	1.80907e-01	1.57225e-02	2.15036e-01
0.241519	1.09194e-03	5.26226e-02	2.95796e-03	5.63867e-02
0.136382	1.53631e-04	1.4597e-02	4.05368e-04	1.44241e-02
0.0714398	2.23882e-05	3.99222e-03	5.7218e-05	3.91765e-03
0.0383488	2.88218e-06	1.00481e-03	8.15548e-06	9.91063e-04
Rate	3.3877	2.2749	3.3502	2.3520
Cubic elements ( $k = 3$ )				
$h$	Dirichlet		Neumann	
	$\ u - u_h\ _{0,\Omega_h}$	$\ u - u_h\ _{1,\Omega_h}$	$\ u - u_h\ _{0,\Omega_h}$	$\ u - u_h\ _{1,\Omega_h}$
0.353553	2.22751e-03	8.49656e-02	9.25961e-03	1.23404e-01
0.241519	1.77764e-04	1.31537e-02	1.31772e-03	1.73723e-02
0.136382	1.41219e-05	1.96634e-03	1.15194e-04	2.17373e-03
0.0714398	1.14619e-06	2.87068e-04	7.63884e-06	2.90969e-04
0.0383488	7.37505e-08	3.61339e-05	6.44114e-07	3.61279e-05
Rate	4.5017	3.3946	4.2777	3.5698
Quartic elements ( $k = 4$ )				
$h$	Dirichlet		Neumann	
	$\ u - u_h\ _{0,\Omega_h}$	$\ u - u_h\ _{1,\Omega_h}$	$\ u - u_h\ _{0,\Omega_h}$	$\ u - u_h\ _{1,\Omega_h}$
0.353553	7.14676e-04	4.08694e-02	2.03226e-03	5.66714e-02
0.241519	3.26085e-05	3.23267e-03	2.85442e-04	4.66504e-03
0.136382	1.77419e-06	2.59726e-04	1.71681e-05	3.17316e-04
0.0714398	7.69598e-08	2.01136e-05	4.39592e-07	2.11306e-05
0.0383488	2.43552e-09	1.27258e-06	2.27363e-08	1.29139e-06
Rate	5.4794	4.5304	5.1745	4.6992

We prove stability and optimal convergence rates  $H^1(\Omega_h)$  and  $L^2(\Omega_h)$  for Dirichlet boundary conditions, while for Neumann boundary conditions our results are restricted to stability and optimal convergence in the  $H^1(\Omega_h)$ -norm.

Numerical tests illustrate the theory and show that optimal convergence rates are also achieved for errors measured in the  $L^2(\Omega_h)$ -norm, even for the case of Neumann boundary conditions.

Future work will explore applications of PE-FEM to other equations and engineering benchmark problems. We will also investigate extensions to boundary operators prescribing, e.g., no slip and no penetration conditions in fluid dynamics. Finally, we will consider problems where the exact curved boundary parameterizations are not known.

TABLE 4. Convergence histories for PE-FEM Dirichlet and Neumann PE-FEM approximations for the flower-shaped domain example. Optimal convergence rates are achieved with respect to both the  $L^2(\Omega_h)$ - and  $H^1(\Omega_h)$ -norms.

Quadratic elements ( $k = 2$ )				
$h$	Dirichlet		Neumann	
	$\ u - u_h\ _{0,\Omega_h}$	$\ u - u_h\ _{1,\Omega_h}$	$\ u - u_h\ _{0,\Omega_h}$	$\ u - u_h\ _{1,\Omega_h}$
0.152981	7.14909e-06	0.000494382	0.00035414	0.000500092
0.130091	3.17824e-06	0.000297894	0.000166025	0.000299439
0.102498	1.50974e-06	0.000179911	8.20902e-05	0.000179586
0.0822541	9.07722e-07	0.000127967	5.02714e-05	0.00012779
0.0743762	6.32287e-07	0.000100181	3.59696e-05	0.000100041
Rate	3.2007	2.1176	3.0260	2.1349
Cubic elements ( $k = 3$ )				
$h$	Dirichlet		Neumann	
	$\ u - u_h\ _{0,\Omega_h}$	$\ u - u_h\ _{1,\Omega_h}$	$\ u - u_h\ _{0,\Omega_h}$	$\ u - u_h\ _{1,\Omega_h}$
0.152981	1.19264e-07	1.20175e-05	1.35612e-05	1.29893e-05
0.130091	4.71919e-08	5.93334e-06	4.72615e-06	6.02536e-06
0.102498	1.76070e-08	2.84338e-06	1.853e-06	2.84707e-06
0.0822541	8.25315e-09	1.634e-06	1.01012e-06	1.64802e-06
0.0743762	4.78806e-09	1.09234e-06	6.34131e-07	1.10467e-06
Rate	4.2805	3.1871	4.0192	3.2610
Quartic elements ( $k = 4$ )				
$h$	Dirichlet		Neumann	
	$\ u - u_h\ _{0,\Omega_h}$	$\ u - u_h\ _{1,\Omega_h}$	$\ u - u_h\ _{0,\Omega_h}$	$\ u - u_h\ _{1,\Omega_h}$
0.152981	1.12437e-09	1.48364e-07	1.27042e-07	2.04383e-07
0.130091	3.76598e-10	6.27032e-08	2.74281e-08	6.75202e-08
0.102498	9.77902e-11	2.12246e-08	2.9125e-09	2.3185e-08
0.0822541	4.04838e-11	1.06185e-08	3.50259e-09	1.11313e-08
0.0743762	2.12426e-11	6.30635e-09	1.41031e-09	6.76371e-09
Rate	5.3364	4.2465	5.8139	4.5229

#### APPENDIX A. ANALYSIS OF TAYLOR POLYNOMIALS ON BOUNDARIES

In this section, we provide technical lemmas pertaining to properties of the Taylor series extensions we have defined in §3.1.

**Lemma 1.** *Let  $v \in L^2(\Omega_h)$ . Then,*

$$\|T_h^k(v)|_{\eta(\xi)}\|_{0,\Gamma_h} \leq C\delta_h^{-\frac{1}{2}}\|v\|_{0,\Omega_h}.$$

*Proof.* We have that  $T_h^k(v)$  is a polynomial on each element domain  $S^{i,\ell}$  so that the  $L^\infty$ -norm on  $\eta(\mathcal{E}_i)$  is bounded by the  $L^\infty$ -norm in  $S^{i,\ell}$ . It then follows that

$$\begin{aligned} \|T_h^k(v)|_{\eta(\xi)}\|_{0,\mathcal{E}_i \cap S^{i,\ell}} &\leq |\mathcal{E}_i \cap S^{i,\ell}|^{\frac{1}{2}} \|T_h^k(v)|_{\eta(\xi)}\|_{L^\infty(\mathcal{E}_i \cap S^{i,\ell})} \\ &\leq C\delta_h^{\frac{d-1}{2}} \|T_h^k(v)|_{\eta}\|_{L^\infty(\eta(\mathcal{E}_i) \cap S^{i,\ell})} \leq C\delta_h^{\frac{d-1}{2}} \|T_h^k(v)\|_{L^\infty(S^{i,\ell})} \end{aligned}$$

because  $\text{diam}(S^{i,\ell}) \leq C\delta_h$ . From [5, Corollary 4.1.15] and after using a scaling argument and noticing that  $\text{diam}(\sigma^{i,\ell}) \leq C\delta_h$ , we have that  $\|T_h^k(v)\|_{L^\infty(S^{i,\ell})} \leq$

$C\delta_h^{-d}\|v\|_{L^1(\sigma^{i,\ell})}$ . It then follows that

$$\begin{aligned} \|T_h^k(v)|_{\boldsymbol{\eta}(\boldsymbol{\xi})}\|_{0,\mathcal{E}_i \cap S^{i,\ell}} &\leq C\delta_h^{-\frac{d+1}{2}}\|v\|_{L^1(\sigma^{i,\ell})} \\ &\leq C\delta_h^{-\frac{d+1}{2}}|\sigma^{i,\ell}|^{\frac{1}{2}}\|v\|_{0,\sigma^{i,\ell}} \leq C\delta_h^{-\frac{1}{2}}\|v\|_{0,\sigma^{i,\ell}}. \end{aligned}$$

We conclude the proof by summing  $\|T_h^k(v)|_{\boldsymbol{\eta}(\boldsymbol{\xi})}\|_{0,\mathcal{E}_i \cap S^{i,\ell}}^2$  over all  $i, \ell$  and noticing that the  $\sigma^{i,\ell}$  are pairwise disjoint.  $\square$

**Lemma 2.** *Let  $U \subset \mathbb{R}^N$  be any domain such that  $\bigcup_{i,j} S^{i,\ell} \subset U$  and  $v \in H^{k+1}(U)$  and let  $m \in \mathbb{N}_0$ . If  $m+1 \leq k$ , then*

$$\|T_h^k(v)|_{\boldsymbol{\eta}(\boldsymbol{\xi})} - v \circ \boldsymbol{\eta}(\boldsymbol{\xi})\|_{m,\Gamma_h} \leq C_{\Omega_h} \delta_h^{k-m+\frac{1}{2}} |v|_{k+1,U}.$$

*Proof.* Recall the Sobolev inequality  $W_p^s(U) \hookrightarrow C(\overline{U})$  if  $s - \frac{d}{p} > 0$ . Because  $k \geq m+1$  and  $d = 2, 3$ , we have that  $v \in W_\infty^m(U)$  and  $D^\alpha v \in C(\overline{U})$  for  $|\alpha| \leq m$ . For  $v \in W_\infty^k(\Omega)$ , Hölder's inequality implies that

$$\|v\|_{m,\Omega} \leq \sqrt{m+1} |\Omega|^{\frac{1}{2}} \|v\|_{W^{m,\infty}(\Omega)}.$$

Therefore, using techniques similar to those used in the proof of Lemma 1, we have that

$$\begin{aligned} \|T_h^k(v)|_{\boldsymbol{\eta}(\boldsymbol{\xi})} - v \circ \boldsymbol{\eta}(\boldsymbol{\xi})\|_{m,\mathcal{E}_i \cap S^{i,\ell}} &\leq \sqrt{m+1} |\mathcal{E}_i \cap S^{i,\ell}|^{\frac{1}{2}} \|T_h^k(v) - v\|_{W_\infty^m(\boldsymbol{\eta}(\mathcal{E}_i) \cap S^{i,\ell})} \\ &\leq C_{\Omega_h,m} \delta_h^{\frac{d-1}{2}} \|T_h^k(v) - v\|_{W_\infty^m(S^{i,\ell})} \\ &\leq C_{\Omega_h,m} \delta_h^{k-m+\frac{1}{2}} |v|_{k+1,S^{i,\ell}}, \end{aligned}$$

where the last inequality follows from [5, Proposition 4.3.2]. We complete the proof by summing the squares of this inequality over  $i, \ell$  and noticing that  $S^{i,\ell}$  are pairwise disjoint.  $\square$

**Remark 7.** If  $U = \mathbb{R}^N$  and  $v \in H^{k+1}(\mathbb{R}^N)$  is an extension of a function  $w \in H^{k+1}(\Omega)$ , then the seminorm  $|v|_{k+1,U}$  in the upper bounds of the inequalities of Lemma 2 can be replaced by  $\|w\|_{k+1,\Omega}$  by virtue of the continuity of the extension operator.

**Lemma 3.** *Let  $v \in L^2(\Omega_h)$  such that  $v|_{\mathcal{K}_n} \in H^{k+1}(\mathcal{K}_n) \cap C^0(\mathcal{K}_n)$  for every  $\mathcal{K}_n \subset \Omega_h$ . Then,*

$$\|T_h^k(v)|_{\boldsymbol{\eta}(\boldsymbol{\xi})} - v(\boldsymbol{\xi})\|_{0,\Gamma_h} \leq C_{\Omega_h} (\delta_h^{\frac{1}{2}} \|v\|_{1,\Omega_h} + \delta_h^{k+\frac{1}{2}} \|v\|_{k+1,\Omega_h}).$$

*Note that, in contrast with Lemma 2,  $v$  is evaluated at  $\boldsymbol{\xi}$  whereas  $T_h^k$  is evaluated at  $\boldsymbol{\eta}(\boldsymbol{\xi})$ .*

*Proof.* Using techniques similar to those used in the proof of Lemma 1, we obtain

$$(36) \quad \|T_h^k(v)|_{\boldsymbol{\eta}(\boldsymbol{\xi})} - v(\boldsymbol{\xi})\|_{0,\Gamma_h} \leq \|T_h^k(v)|_{\boldsymbol{\xi}} - v(\boldsymbol{\xi})\|_{0,\Gamma_h} + \|T_h^k(v)|_{\boldsymbol{\eta}(\boldsymbol{\xi})} - T_h^k(v)|_{\boldsymbol{\xi}}\|_{0,\Gamma_h}.$$

To bound the first term on the right-hand side of (36) we proceed as in the proof of Lemma 2, but now working on the domains  $S^{i,\ell} \cap \mathcal{K}_{j_i}$  (which are still star-shaped with respect to  $\sigma^{i,\ell}$ ) instead of  $S^{i,\ell}$ . Also, because  $v \notin H^{k+1}(\Omega_h)$ , we must instead bound the error by a broken norm, e.g., we have that

$$\|T_h^k(v)|_{\boldsymbol{\xi}} - v(\boldsymbol{\xi})\|_{0,\Gamma_h} \leq C\delta_h^{k+\frac{1}{2}} \|v\|_{k+1,\Omega_h}.$$

On each  $S^{i,\ell}$ , the second term on the right-hand side of (36) features the difference of the same polynomial evaluated at the different points  $\boldsymbol{\eta}(\boldsymbol{\xi})$  and  $\boldsymbol{\xi}$ . Hence, using the classical first-order Taylor expansion on the polynomial, we have, for  $\boldsymbol{\xi}, \boldsymbol{\eta}(\boldsymbol{\xi}) \in S^{i,\ell}$ ,

$$\begin{aligned} \|T_h^k(v)|_{\boldsymbol{\eta}(\boldsymbol{\xi})} - T_h^k(v)|_{\boldsymbol{\xi}}\|_{\mathcal{E}_i \cap S^{i,\ell}} &= \|\nabla T_h^k(v)|_{\boldsymbol{\xi}'}(\boldsymbol{\eta}(\boldsymbol{\xi}) - \boldsymbol{\xi})\|_{\mathcal{E}_i \cap S^{i,\ell}} \\ &\leq C\delta_h \|\mathbf{T}_h^{k-1}(\nabla v)|_{\boldsymbol{\xi}}\|_{\mathcal{E}_i \cap S^{i,\ell}} \leq C\delta_h^{\frac{1}{2}} \|\nabla v\|_{0,\sigma^{i,\ell}}, \end{aligned}$$

where  $\boldsymbol{\xi}' = t\boldsymbol{\xi} + (1-t)\boldsymbol{\eta}(\boldsymbol{\xi})$  for some  $t \in [0, 1]$ . For the first inequality we used the fact that, on each  $S^{i,\ell}$ ,  $D^\alpha T_h^k(v) = T_h^{k-|\alpha|}(D^\alpha v)$ ; see [5, Proposition 4.1.17]. For the last inequality we proceeded as in the proof of Lemma 1.  $\square$

**Lemma 4.** *If  $v \in \overline{V}_h^k$ , then*

$$(37) \quad \|T_h^{k',k}(v)|_{\boldsymbol{\eta}(\boldsymbol{\xi})}\|_{0,\Gamma_h} \leq C_{\Omega,k} \left( \sum_{|\boldsymbol{\alpha}|=k'}^k h^{-|\boldsymbol{\alpha}|-1/2} \delta_h^{|\boldsymbol{\alpha}|} \right) \|v\|_{0,\Omega_h}.$$

*In addition, if  $v \in V_h^k$  and  $m > 0$ , then*

$$(38) \quad \|T_h^{k',k}(v)|_{\boldsymbol{\eta}(\boldsymbol{\xi})}\|_{0,\Gamma_h} \leq C_{\Omega,k} \left( \sum_{|\boldsymbol{\alpha}|=k'}^k h^{-|\boldsymbol{\alpha}|+1/2} \delta_h^{|\boldsymbol{\alpha}|} \right) |v|_{1,\Omega_h}.$$

*Proof.* Let  $v \in \overline{V}_h^k$ . Then it follows from the definition of  $T_h^{k',k}(\cdot)$  that

$$\begin{aligned} \|T_h^{k',k}(v)|_{\boldsymbol{\eta}(\boldsymbol{\xi})}\|_{0,\mathcal{E}_i} &= \left\| \sum_{|\boldsymbol{\alpha}|=k'}^k \frac{1}{\boldsymbol{\alpha}!} D_h^\boldsymbol{\alpha} v(\boldsymbol{\xi}) |\boldsymbol{\xi} - \boldsymbol{\eta}(\boldsymbol{\xi})|^\boldsymbol{\alpha} \right\|_{0,\mathcal{E}_i} \\ &\leq \sum_{|\boldsymbol{\alpha}|=k'}^k \delta_h^{|\boldsymbol{\alpha}|} \frac{1}{\boldsymbol{\alpha}!} \|D_h^\boldsymbol{\alpha} v(\boldsymbol{\xi})\|_{0,\mathcal{E}_i} \leq Ch^{\frac{d-1}{2}} \sum_{|\boldsymbol{\alpha}|=k'}^k \delta_h^{|\boldsymbol{\alpha}|} \frac{1}{\boldsymbol{\alpha}!} \|D_h^\boldsymbol{\alpha} v\|_{L^\infty(\mathcal{E}_i)} \\ &\leq Ch^{\frac{d-1}{2}} \sum_{|\boldsymbol{\alpha}|=k'}^k \delta_h^{|\boldsymbol{\alpha}|} \frac{1}{\boldsymbol{\alpha}!} \|D_h^\boldsymbol{\alpha} v\|_{L^\infty(\mathcal{K}_{j_i})} \leq Ch^{-\frac{1}{2}} \sum_{|\boldsymbol{\alpha}|=k'}^k \delta_h^{|\boldsymbol{\alpha}|} \frac{1}{\boldsymbol{\alpha}!} \|D_h^\boldsymbol{\alpha} v\|_{0,\mathcal{K}_{j_i}}. \end{aligned}$$

Using the inverse inequality we have that

$$\|T_h^{k',k}(v)|_{\boldsymbol{\eta}(\boldsymbol{\xi})}\|_{0,\mathcal{E}_i} \leq Ch^{-\frac{1}{2}} \sum_{|\boldsymbol{\alpha}|=1}^k h^{-|\boldsymbol{\alpha}|} \delta_h^{|\boldsymbol{\alpha}|} \frac{1}{\boldsymbol{\alpha}!} \|v\|_{0,\mathcal{K}_{j_i}}$$

so that (37) follows by summing the terms  $\|T_h^k(v)|_{\boldsymbol{\eta}(\boldsymbol{\xi})} - v(\boldsymbol{\xi})\|_{0,\mathcal{E}_i}^2$ .

For  $m > 0$ , we can write

$$\begin{aligned} \|T_h^{k',k}(v)|_{\boldsymbol{\eta}(\boldsymbol{\xi})}\|_{0,\mathcal{E}_i} &\leq Ch^{-\frac{1}{2}} \sum_{|\boldsymbol{\alpha}|=k'}^k \delta_h^{|\boldsymbol{\alpha}|} \frac{1}{\boldsymbol{\alpha}!} \|D_h^\boldsymbol{\alpha} v\|_{0,\mathcal{K}_{j_i}} \\ &\leq Ch^{-\frac{1}{2}} \sum_{|\boldsymbol{\alpha}|=k'}^k h^{1-|\boldsymbol{\alpha}|} \delta_h^{|\boldsymbol{\alpha}|} \frac{1}{\boldsymbol{\alpha}!} |v|_{1,\mathcal{K}_{j_i}}, \end{aligned}$$

where for the last inequality we used the fact that  $D^\boldsymbol{\alpha} v = D^{\beta_\boldsymbol{\alpha}}(\partial_{x_{i_\boldsymbol{\alpha}}} v)$  for some  $\beta_\boldsymbol{\alpha}$  such that  $|\beta_\boldsymbol{\alpha}| = |\boldsymbol{\alpha}| - 1$  and some  $i_\boldsymbol{\alpha} \in \{1, \dots, d\}$ . Hence,

$$\|D^\boldsymbol{\alpha} v\|_{0,\Omega_h} = \|D^{\beta_\boldsymbol{\alpha}}(\partial_{x_{i_\boldsymbol{\alpha}}} v)\|_{0,\Omega_h} \leq Ch^{-|\beta_\boldsymbol{\alpha}|} \|\partial_{x_{i_\boldsymbol{\alpha}}} v\|_{0,\Omega_h} \leq Ch^{1-|\boldsymbol{\alpha}|} |v|_{1,\Omega_h}$$

so that (38) follows by summing the square of these terms.  $\square$

**Lemma 5.** Let  $v \in L^2(\Omega_h)$  and  $v|_{\mathcal{K}_n} \in H^2(\mathcal{K}_n)$  for every  $\mathcal{K}_n \subset \Omega_h$ . Then,

$$\|v\|_{0,\Gamma_h} \leq C_{\Omega_h}(h^{-\frac{1}{2}}\|v\|_{0,\Omega_h} + h^{\frac{3}{2}}\|v\|_{2,\Omega_h}).$$

*Proof.* Letting  $Q_i^1(u)$  denote the averaged Taylor polynomial of degree 1 defined on the maximal ball included in  $\mathcal{K}_{j_i}$ , we have

$$\begin{aligned} \|v\|_{0,\mathcal{E}_i} &\leq C|\mathcal{E}_i|^{\frac{1}{2}}\|v\|_{L^\infty(\mathcal{E}_i)} \leq Ch^{\frac{d-1}{2}}\|v\|_{L^\infty(\mathcal{K}_{j_i})} \\ &\leq Ch^{\frac{d-1}{2}}(\|v - Q_i^1 v\|_{L^\infty(\mathcal{K}_{j_i})} + \|Q_i^1 v\|_{L^\infty(\mathcal{K}_{j_i})}) \\ &\leq Ch^{\frac{d-1}{2}}(h^{2-\frac{d}{2}}\|v\|_{2,\mathcal{K}_{j_i}} + h^{-d}\|v\|_{L^1(\mathcal{K}_{j_i})}) \leq Ch^{\frac{3}{2}}\|v\|_{2,\mathcal{K}_{j_i}} + Ch^{-\frac{1}{2}}\|v\|_{0,\mathcal{K}_{j_i}}, \end{aligned}$$

where for the fourth inequality we have used [5, Corollary 4.1.13] and [5, Proposition 4.3.2] on the domain  $\mathcal{K}_{j_i}$  which is star shaped with respect to  $\sigma^{i,\ell}$ .  $\square$

## APPENDIX B. ANALYSIS OF EXTENSION ERROR

In this section, we present results pertaining to the error between different extensions of a function in  $H^k(\Omega)$  into  $H^k(\Omega_h)$ .

**Lemma 6.** Let  $f \in H^k(\Omega)$  and let  $\tilde{f}$  and  $\bar{f}$  denote two extensions of  $f$  in  $H^k(\mathbb{R}^N)$  such that  $\|\tilde{f}\|_{k,\mathbb{R}^N} \leq C\|f\|_{k,\Omega}$  and  $\|\bar{f}\|_{k,\mathbb{R}^N} \leq C\|f\|_{k,\Omega}$ . Then, for  $m, k \in \mathbb{Z}$  such that  $0 \leq m \leq k$ ,

$$\|\tilde{f} - \bar{f}\|_{m,\Omega_h} = C_{k,d}\delta_h^{k-m}\|f\|_{k,\Omega}.$$

*Proof.* Because  $\tilde{f} = \bar{f} = f$  in  $\Omega$ ,

$$\|\tilde{f} - \bar{f}\|_{k,\Omega_h} \leq \|\tilde{f} - \bar{f}\|_{k,\Omega_h \setminus (\Omega \cap \Omega_h)}.$$

Using the Bramble-Hilbert lemma (see [5, Lemma 4.3.8]), we have

$$\begin{aligned} \|\tilde{f} - T_h^{k-1}f\|_{m,\Omega_h \setminus (\Omega \cap \Omega_h)}^2 &\leq \sum_{i,j} \|\tilde{f} - T_h^{k-1}f\|_{m,S^{i,\ell}}^2 \leq C_{k,d} \sum_{i,j} \delta_h^{2(k-m)} |\tilde{f}|_{k,S^{i,\ell}}^2 \\ &\leq C_{k,d} \delta_h^{2(k-m)} |\tilde{f}|_{k,\mathbb{R}^N}^2 \leq C_{k,d} \delta_h^{2(k-m)} \|f\|_{k,\Omega}^2. \end{aligned}$$

Therefore

$$\|\tilde{f} - T_h^{k-1}f\|_{m,\Omega_h} \leq C_{k,d}\delta_h^{k-m}\|f\|_{k,\Omega},$$

which holds for  $\bar{f}$  in place of  $\tilde{f}$  as well. The lemma follows from noticing that

$$\|\tilde{f} - \bar{f}\|_{m,\Omega_h} \leq \|\tilde{f} - T_h^{k-1}f\|_{m,\Omega_h} + \|\bar{f} - T_h^{k-1}f\|_{m,\Omega_h}.$$

$\square$

**Lemma 7.** Let  $f$ ,  $\tilde{f}$ , and  $\bar{f}$  be as in Lemma 6. Then,

$$|\langle \tilde{f} - \bar{f}, v \rangle_{\Omega_h}| \leq C_{k,d}\delta_h^{k+\frac{1}{2}-\frac{1}{q}}\|f\|_{k,\Omega}\|v\|_{1,\Omega_h} \quad \forall v \in H^1(\Omega_h)$$

for  $0 \leq m \leq k$  and  $2 \leq q < 6$  if  $\Omega_h \subset \mathbb{R}^3$  and  $2 \leq q < \infty$  if  $\Omega_h \subset \mathbb{R}^2$ .

*Proof.* Let  $\Omega_h^{\text{diff}} := \Omega_h \setminus (\Omega \cap \Omega_h)$  and note that  $|\Omega_h^{\text{diff}}| \sim O(\delta_h)$ . Because  $H^1(\Omega_h)$  is compactly embedded in  $L^q(\Omega_h)$ , we have, for  $p = (\frac{1}{2} - \frac{1}{q})^{-1}$ ,

$$\begin{aligned} |\langle \tilde{f} - \bar{f}, v \rangle_{\Omega_h}| &= \left| \left\langle \tilde{f} - \bar{f}, v \right\rangle_{\Omega_h} \right|_{\Omega_h^{\text{diff}}} \leq \|\tilde{f} - \bar{f}\|_{0,\Omega_h^{\text{diff}}} \|v\|_{L^q(\Omega_h^{\text{diff}})} \|1\|_{L^p(\Omega_h^{\text{diff}})} \\ &\leq C_{k,d} \delta_h^k \|f\|_{k,\Omega} \|v\|_{L^q(\Omega_h)} |\Omega_h^{\text{diff}}|^{\frac{1}{p}} \leq C_{k,d} \delta_h^{k+\frac{1}{p}} \|f\|_{k,\Omega} \|v\|_{1,\Omega_h}, \end{aligned}$$

where for the second inequality we used Lemma 6.  $\square$

APPENDIX C. CONTINUITY OF THE  $L^2$  PROJECTION IN  $H^{\frac{1}{2}}$ 

In this section, we analyze the stability of the  $L^2$  projection operator in the  $H^{1/2}(\Gamma_h)$  topology.

**Lemma 8.** *Let  $\pi_h : L^2(\Gamma_h) \rightarrow W_h^k$  be the  $L^2(\Gamma_h)$  projection from  $L^2(\Gamma_h)$  into the discrete trace approximation space. Then, for all  $w \in H^{1/2}(\Gamma_h)$ , we have that*

$$\|\pi_h w\|_{1/2,\Gamma_h} \leq C \|w\|_{1/2,\Gamma_h},$$

where the constant  $C$  does not depend on the mesh size  $h$ .

*Proof.* The projection operator  $\pi_h$  is linear and maps  $H^0(\Gamma_h)$  to  $H^0(\Gamma_h)$  and  $H^1(\Gamma_h)$  to  $H^1(\Gamma_h)$ . Furthermore, for  $v_0 \in H^0(\Gamma_h)$  and  $v_1 \in H^1(\Gamma_h)$ , we have that  $\|\pi_h(v_0)\|_{0,\Gamma_h} \leq C_0 \|v_0\|_{0,\Gamma_h}$  and  $\|\pi_h(v_1)\|_{1,\Gamma_h} \leq C_1 \|v_1\|_{1,\Gamma_h}$ ; see [18, Lemma 1.131]. Using the operator interpolation theory and in particular [5, Proposition 14.1.5], we have that  $\pi_h$  maps  $H^{1/2}(\Gamma_h)$  to  $H^{1/2}(\Gamma_h)$  and that its norm satisfies

$$\|\pi_h\|_{H^{1/2} \rightarrow H^{1/2}} \leq \|\pi_h\|_{H^0 \rightarrow H^0}^{\frac{1}{2}} \|\pi_h\|_{H^1 \rightarrow H^1}^{\frac{1}{2}} \leq \sqrt{C_0 C_1}.$$

Hence, for  $w \in H^{1/2}(\Gamma_h)$  we have

$$\|\pi_h w\|_{1/2,\Gamma_h} \leq \|\pi_h\|_{H^{1/2} \rightarrow H^{1/2}} \|w\|_{1/2,\Gamma_h} \leq \sqrt{C_0 C_1} \|w\|_{1/2,\Gamma_h}.$$

□

## APPENDIX D. PROOFS OF WELL-POSEDNESS RESULTS

**D.1. Proof of Theorem 1.** The bound (27) for  $u, v \in V_h^k$  is derived simply by seeing that

$$\begin{aligned} B_{h,D}^\theta(u, v) &= D_h(u, v - \mathcal{R}_h v_\star) + \theta_h \langle T_h^k(u)|_{\boldsymbol{\eta}(\boldsymbol{\xi})}, v \rangle_{\Gamma_h} \\ &\leq C_{\mathcal{R}_h} \bar{p} |u|_{1,\Omega_h} \|v\|_{1,\Omega_h} + \theta_h \|T_h^k(u)|_{\boldsymbol{\eta}(\boldsymbol{\xi})}\|_{0,\Gamma_h} |v|_{1,\Omega_h} \\ &\leq C \left( \bar{p} + \theta_h \left( 1 + \sum_{|\boldsymbol{\alpha}|=1}^k h^{\frac{1}{2}-|\boldsymbol{\alpha}|} \delta_h^{|\boldsymbol{\alpha}|} \right) \right) \|u\|_{1,\Omega_h} \|v\|_{1,\Omega_h}, \end{aligned}$$

where use is made of the trace inequality and Lemma 4.

To show that (28) holds under the hypotheses of the theorem, note that, after applying Lemma 4, we have

$$\begin{aligned} \langle T_h^k(u)|_{\boldsymbol{\eta}(\boldsymbol{\xi})}, u \rangle_{\Gamma_h} &= \int_{\Gamma_h} u^2 ds + \langle T_h^k(u)|_{\boldsymbol{\eta}(\boldsymbol{\xi})} - u, u \rangle_{\Gamma_h} \\ &\geq \|u\|_{0,\Gamma_h}^2 - \|T_h^{1,k}(u)|_{\boldsymbol{\eta}(\boldsymbol{\xi})}\|_{0,\Gamma_h} \|u\|_{0,\Gamma_h} \\ &\geq \|u\|_{0,\Gamma_h}^2 - C \left( \sum_{|\boldsymbol{\alpha}|=1}^k h^{\frac{1}{2}-|\boldsymbol{\alpha}|} \delta_h^{|\boldsymbol{\alpha}|} \right) |u|_{1,\Omega_h} \|u\|_{0,\Gamma_h}. \end{aligned}$$

Second, after applying the Cauchy-Schwarz inequality, Young's inequality, and the inverse inequality, we have that

$$\begin{aligned} D_h(u, u - \mathcal{R}_h u_\star) &= D_h(u, u) - D_h(u, \mathcal{R}_h u_\star) \\ &\geq \underline{p} |u|_{1,\Omega_h}^2 - \bar{p} \|\mathcal{R}_h\| |u|_{1,\Omega_h} \|u\|_{1/2,\Gamma_h} \geq \frac{3}{4} \underline{p} |u|_{1,\Omega_h}^2 - \frac{C_{inv} \bar{p} \|\mathcal{R}_h\|}{ph} \|u\|_{0,\Gamma_h}^2. \end{aligned}$$

We then have that

$$\begin{aligned} B_{h,D}^\theta(u,u) &\geq \frac{3}{4}\underline{p}|u|_{1,\Omega_h}^2 + \left(\theta_h - \frac{C_{inv}\bar{p}\|\mathcal{R}_h\|}{ph}\right)\|u\|_{0,\Gamma_h}^2 \\ &\quad - C\theta_h \left(\sum_{|\alpha|=1}^k h^{\frac{1}{2}-|\alpha|}\delta_h^{|\alpha|}\right)|u|_{1,\Omega_h}\|u\|_{0,\Gamma_h}. \end{aligned}$$

If we assume that  $\theta_h = \frac{C_\theta}{h}$  with  $C_\theta \geq \frac{C_{inv}\bar{p}\|\mathcal{R}_h\|}{\underline{p}}$ , we have by Friedrich's inequality

$$\frac{3}{4}\underline{p}|u|_{1,\Omega_h}^2 + \left(\theta_h - \frac{C_{inv}\bar{p}\|\mathcal{R}_h\|}{ph}\right)\|u\|_{0,\Gamma_h}^2 \geq c\|u\|_{1,\Omega_h}^2;$$

see [18, Lemma B.63]. Hence

$$B_{h,D}^\theta(u,u) \geq c\|u\|_{1,\Omega_h}^2 - CC_\theta \left(\sum_{|\alpha|=1}^k h^{-\frac{1}{2}-|\alpha|}\delta_h^{|\alpha|}\right)|u|_{1,\Omega_h}\|u\|_{0,\Gamma_h}.$$

The coercivity condition (28) is achieved given  $\delta_h \sim o(h^{\frac{3}{2}})$  and  $h$  small enough.

We now prove the stability bound (29). Let  $u_h$  denote the solution to (18) and let  $\pi_h : L^2(\Gamma_h) \rightarrow W_h^k$  denote the  $L^2(\Gamma_h)$  projection operator onto  $W_h^k$ . Equation (18)<sub>2</sub> is equivalent to

$$u_h(\xi) = \pi_h[g_D \circ \eta(\xi)] - \pi_h[T_h^{1,k}(u)|_{\eta(\xi)}].$$

Because of this we have that

$$\begin{aligned} \|u_h\|_{1/2,\Gamma_h} &\leq \|\pi_h[g_D \circ \eta(\xi)]\|_{1/2,\Gamma_h} + \left\|\pi_h[T_h^{1,k}(u_h)|_{\eta(\xi)}]\right\|_{1/2,\Gamma_h} \\ &\leq \|\pi_h[g_D \circ \eta(\xi)]\|_{1/2,\Gamma_h} + Ch^{-\frac{1}{2}} \left\|\pi_h[T_h^{1,k}(u_h)|_{\eta(\xi)}]\right\|_{0,\Gamma_h} \\ (39) \quad &\leq C \left( \left\|g_D \circ \eta(\xi)\right\|_{1/2,\Gamma_h} + h^{-\frac{1}{2}} \left\|T_h^{1,k}(u_h)|_{\eta(\xi)}\right\|_{0,\Gamma_h} \right) \\ &\leq C \left( \left\|g_D \circ \eta(\xi)\right\|_{1/2,\Gamma_h} + \left( \sum_{|\alpha|=1}^k h^{-|\alpha|-\frac{1}{2}} \delta_h^{|\alpha|} \right) |u_h|_{1,\Omega_h} \right) \end{aligned}$$

after utilizing the inequality  $\|\pi_h w\|_{1/2,\Gamma_h} \leq C\|w\|_{1/2,\Gamma_h}$ ; see Lemma 8, Lemma 4, and the inverse inequality.

Consider now that

$$\begin{aligned} (40) \quad &\underline{p}|u_h|_{1,\Omega_h}^2 - \bar{p}\|\mathcal{R}_h\||u_h|_{1,\Omega_h}\|u_h\|_{1/2,\Gamma_h} \\ &\leq D_h(u_h, u_h - \mathcal{R}_h(u_h)_*) = \langle \tilde{f}, u_h - \mathcal{R}_h(u_h)_* \rangle_{\Omega_h}. \end{aligned}$$

From this we obtain

$$(41) \quad |u_h|_{1,\Omega_h}^2 \leq C(\|\tilde{f}\|_{-1,\Omega_h} + \|u_h\|_{1/2,\Gamma_h})\|u_h\|_{1,\Omega_h}.$$

Adding  $\|u_h\|_{1/2,\Gamma_h}^2$  to both sides of the inequality, using the trace inequality, and redefining the constant  $C$ , we obtain

$$|u_h|_{1,\Omega_h}^2 + \|u_h\|_{1/2,\Gamma_h}^2 \leq C(\|\tilde{f}\|_{-1,\Omega_h} + \|u_h\|_{1/2,\Gamma_h})\|u_h\|_{1,\Omega_h}.$$

We have that  $\|u_h\|_{1,\Omega_h}^2 \leq C(|u_h|_{1,\Omega_h}^2 + \|u_h\|_{1/2,\Gamma_h}^2)$ ; see Thanks to [18, Lemma B.63]. Therefore,

$$\|u_h\|_{1,\Omega_h} \leq C(\|\tilde{f}\|_{-1,\Omega_h} + \|u_h\|_{1/2,\Gamma_h}).$$

Subsequently substituting  $\|u_h\|_{1/2,\Gamma_h}$  for its upper bound in (39) yields

$$\|u_h\|_{1,\Omega_h} - C \left( \sum_{|\alpha|=1}^k h^{-|\alpha|-\frac{1}{2}} \delta_h^{|\alpha|} \right) \|u_h\|_{1,\Omega_h} \leq C \left( \|\tilde{f}\|_{-1,\Omega_h} + \|g_D \circ \boldsymbol{\eta}(\boldsymbol{\xi})\|_{1/2,\Gamma_h} \right).$$

It then follows that (29) is satisfied if  $\delta_h \sim o(h^{\frac{3}{2}})$  and  $h$  is small enough.

**D.2. Proof of Theorem 2.** Recall that  $B_{h,N}(u, v) = N_h(u, v) + \boldsymbol{\tau}_N(u, v)$ , where

$$\boldsymbol{\tau}_N(u, v) := \langle \tilde{p} \circ \boldsymbol{\eta}(\boldsymbol{\xi}) \mathbf{T}_h^{k-1}(\nabla u) \Big|_{\boldsymbol{\eta}(\boldsymbol{\xi})} \cdot \mathbf{n} - \tilde{p}(\boldsymbol{\xi}) \nabla u \cdot \mathbf{n}_h, v \rangle_{\Gamma_h}.$$

We have

$$\begin{aligned} |\boldsymbol{\tau}_N(u, v)| &\leq \left| \langle (\tilde{p} \circ \boldsymbol{\eta}(\boldsymbol{\xi}) - \tilde{p}(\boldsymbol{\xi})) \nabla u \cdot \mathbf{n}_h, v \rangle_{\Gamma_h} \right| + \left| \langle \tilde{p} \circ \boldsymbol{\eta}(\boldsymbol{\xi}) \nabla u \cdot (\mathbf{n} - \mathbf{n}_h), v \rangle_{\Gamma_h} \right| \\ &\quad + \left| \langle \tilde{p} \circ \boldsymbol{\eta}(\boldsymbol{\xi}) (\mathbf{T}_h^{k-1}(\nabla u) \Big|_{\boldsymbol{\eta}(\boldsymbol{\xi})} - \nabla u) \cdot \mathbf{n}, v \rangle_{\Gamma_h} \right|. \end{aligned}$$

Because  $|\tilde{p}(\boldsymbol{\eta}(\boldsymbol{\xi})) - \tilde{p}(\boldsymbol{\xi})| \leq C\delta_h \|\tilde{p}\|_{C^1(\overline{\Omega}_h)}$  and  $|\tilde{p}(\boldsymbol{\eta}(\boldsymbol{\xi}))(\mathbf{n} - \mathbf{n}_h)| \leq Ch \|\tilde{p}\|_{C^0(\overline{\Omega}_h)}$ , we have that

$$\begin{aligned} (42) \quad |\boldsymbol{\tau}_N(u, v)| &\leq C_p (\delta_h + h) \|\nabla u\|_{0,\Gamma_h} \|v\|_{0,\Gamma_h} \\ &\quad + C_p \left\| \mathbf{T}_h^{k-1}(\nabla u) \Big|_{\boldsymbol{\eta}(\boldsymbol{\xi})} - \nabla u \right\|_{0,\Gamma_h} \|v\|_{0,\Gamma_h}. \end{aligned}$$

Lemma 5 implies that  $\|\nabla u\|_{0,\Gamma_h} \leq Ch^{-\frac{1}{2}} \|\nabla u\|_{0,\Omega_h} + h^{\frac{3}{2}} \|\nabla u\|_{2,\Omega_h}$ . Combining this with Lemma 3 yields the upper bound

$$\begin{aligned} |\boldsymbol{\tau}_N(u, v)| &\leq C \left[ (\delta_h h^{-\frac{1}{2}} + h^{\frac{1}{2}}) \|\nabla u\|_{0,\Omega_h} + (\delta_h h^{\frac{3}{2}} + h^{\frac{5}{2}}) \|\nabla u\|_{2,\Omega_h} \right. \\ &\quad \left. + \delta_h^{\frac{1}{2}} \|\nabla u\|_{1,\Omega_h} + \delta_h^{k-\frac{1}{2}} \|\nabla u\|_{k,\Omega_h} \right] \|v\|_{0,\Gamma_h}, \end{aligned}$$

where (33) is derived considering that  $B_{h,N}(u, v) = N_h(u, v) + \boldsymbol{\tau}_N(u, v)$ ,  $N_h(u, v) \leq M \|u\|_{1,\Omega_h} \|v\|_{1,\Omega_h}$ , and the assumption that  $\delta_h \sim o(h^{\frac{3}{2}})$ .

If  $u \in V_h^k$ , the discrete continuity bound (30) is derived by proceeding as in the above paragraph but now using Lemma 4 in (42) to see that

$$\begin{aligned} (43) \quad \left\| \mathbf{T}_h^{k-1}(\nabla u) \Big|_{\boldsymbol{\eta}(\boldsymbol{\xi})} - \nabla u \right\|_{0,\Gamma_h} &= \left\| \mathbf{T}_h^{1,k-1}(\nabla u) \Big|_{\boldsymbol{\eta}(\boldsymbol{\xi})} \right\|_{0,\Gamma_h} \\ &\leq C_P \left( \sum_{|\alpha|=1}^k h^{-\frac{1}{2}-|\alpha|} \delta_h^{|\alpha|} \right) \leq C \|u\|_{0,\Omega_h}, \end{aligned}$$

given that  $\delta_h \sim o(h^{\frac{3}{2}})$ .

We now show that (31) holds. We have that

$$(44) \quad N_h(u, u) \geq C_{\underline{p}, \underline{q}} \|u\|_{1,\Omega_h}^2 \quad \forall u \in V_h^k,$$

where  $C_{\underline{p}, \underline{q}} = \min(\underline{p}, \underline{q})$ . Using (44), the discrete bound on  $|\boldsymbol{\tau}_N(u, v)|$  (i.e., (42) with (43)), and the discrete trace inequality  $\|v\|_{0,\Gamma_h} \leq Ch^{-\frac{1}{2}} \|v\|_{0,\Omega_h}$  for all  $v \in V_h^k$ , yields

$$B_{h,N}(u, u) \geq \left[ C_{\underline{p}, \underline{q}} - C_{\overline{p}} \left( (\delta_h h^{-\frac{1}{2}} + h^{\frac{1}{2}}) + \sum_{|\alpha|=1}^k h^{-\frac{1}{2}-|\alpha|} \delta_h^{|\alpha|} \right) \right] \|u\|_{1,\Omega_h}^2$$

for all  $u \in V_h^k$ . This implies (31) if  $\delta_h \sim o(h^{\frac{3}{2}})$ .

Finally, using (31), one obtains

$$\begin{aligned}\|u_h\|_{1,\Omega_h}^2 &\leq \gamma_N^{-1} B_{h,N}(u_h, u_h) = \gamma_N^{-1} (F_h(u_h) + \langle g_N \circ \boldsymbol{\eta}(\boldsymbol{\xi}), u_h \rangle_{\Gamma_h}) \\ &\leq C \gamma_N^{-1} (\|\tilde{f}\|_{-1,\Omega_h} + \|g_N \circ \boldsymbol{\eta}(\boldsymbol{\xi})\|_{-1/2,\Gamma_h}) \|u_h\|_{1,\Omega_h}\end{aligned}$$

and hence (32) is satisfied.

#### APPENDIX E. PROOFS OF ERROR ESTIMATES

In this section, we provide the proofs of the error estimates given in Theorems 3, 4, and 5.

**E.1. Proof of Theorem 3.** We assume that (5) has a solution  $u \in H^{k+1}(\Omega)$  with an extension  $\tilde{u} \in H^{k+1}(\mathbb{R}^N)$ . We let  $\hat{f} = L_D \tilde{u}$ , where  $L_D$  denotes the strong operator in (3). The error analysis follows the familiar strategy of breaking up  $u_h$  into a sum of an interpolant  $u_I \in V_h^k$  of  $\tilde{u}$  and a discrete error term  $w_h = u_h - u_I$ . We start with a preliminary result that is central to showing optimal convergence in the  $H^1(\Omega_h)$ -norm.

**Lemma 9.** *Let  $u_h \in V_h^k$  denote the solution of the Dirichlet PE-FEM problem (18) and assume that  $g_D \circ \boldsymbol{\eta}(\boldsymbol{\xi}) \in L^2(\Gamma_h)$ . Then, we have the stability bound*

$$(45) \quad \|u_h\|_{1,\Omega_h} \leq C (\|\tilde{f}\|_{-1,\Omega_h} + h^{-\frac{1}{2}} \|g_D \circ \boldsymbol{\eta}(\boldsymbol{\xi})\|_{0,\Gamma_h}).$$

*Proof.* From (40) we deduce that

$$\underline{p}|u_h|_{1,\Omega_h}^2 - C\bar{p}|u_h|_{1,\Omega_h} \|u_h\|_{1/2,\Gamma_h} \leq C\|\tilde{f}\|_{-1,\Omega_h} \|u_h\|_{1,\Omega_h}.$$

Applying the inverse inequality and Cauchy's inequality gives us

$$(46) \quad \frac{p}{2}|u_h|_{1,\Omega_h}^2 - \frac{Ch^{-1}}{2p} \|u_h\|_{0,\Gamma_h}^2 \leq C\|\tilde{f}\|_{-1,\Omega_h} \|u_h\|_{1,\Omega_h}.$$

Because we have that

$$u_h|_{\Gamma_h} = \pi_h [g_D \circ \boldsymbol{\eta}(\boldsymbol{\xi}) - T_h^{1,k}(u_h)|_{\boldsymbol{\eta}(\boldsymbol{\xi})}],$$

where  $\pi_h(\cdot) : L^2(\Gamma_h) \rightarrow W_h^k$  is the  $L^2(\Gamma_h)$  projection operator into  $W_h^k$ , it follows from Lemma 4 and the continuity of the projection operator in the  $L^2(\Gamma_h)$  topology that

$$(47) \quad \|u_h\|_{0,\Gamma_h} \leq C \sum_{|\boldsymbol{\alpha}|=1} h^{-|\boldsymbol{\alpha}|+\frac{1}{2}} \delta_h^{|\boldsymbol{\alpha}|} |u_h|_{1,\Omega_h} + C \|g_D \circ \boldsymbol{\eta}(\boldsymbol{\xi})\|_{0,\Gamma_h}.$$

Inserting this inequality into (46) yields

$$\left( \frac{p^2}{4} - \left( C \sum_{|\boldsymbol{\alpha}|=1} h^{-|\boldsymbol{\alpha}|} \delta_h^{|\boldsymbol{\alpha}|} \right)^2 \right) |u_h|_{1,\Omega_h}^2 \leq C\|\tilde{f}\|_{-1,\Omega_h} \|u_h\|_{1,\Omega_h} + \frac{Ch^{-1}}{2p} \|g_D \circ \boldsymbol{\eta}(\boldsymbol{\xi})\|_{0,\Gamma_h}^2.$$

Adding (47) to this inequality and subsequently using Friedrich's inequality (i.e.,  $C\|u\|_{1,\Omega_h}^2 \leq \|u\|_{0,\Gamma_h}^2 + |u|_{1,\Omega_h}^2$ ) and the Cauchy inequality yields

$$\|u_h\|_{1,\Omega_h}^2 \leq C (\|\tilde{f}\|_{-1,\Omega_h}^2 + h^{-1} \|g_D \circ \boldsymbol{\eta}(\boldsymbol{\xi})\|_{0,\Gamma_h}^2)$$

after applying the assumption that  $\delta_h \sim o(h)$ .  $\square$

We proceed with the main result.

*Proof of Theorem 3.* Application of the triangle inequality yields an error bound

$$(48) \quad \|\tilde{u} - u_h\|_{1,\Omega_h} \leq \|\tilde{u} - u_I\|_{1,\Omega_h} + \|w_h\|_{1,\Omega_h}$$

in terms of the *interpolation error* and the *discrete error*, where  $w_h = u_h - u_I$ . Standard interpolation results imply optimal convergence of the first term. Thus, to complete the proof it remains to show that the discrete error is also optimal. By linearity,  $w_h \in V_h^k$  satisfies the equation

$$\begin{aligned} B_{h,D}^\theta(w_h, v) &= \left\langle \tilde{f} - [-\nabla \cdot (\tilde{p}(x)\nabla u_I)], v - \mathcal{R}_h v_\star \right\rangle_{\Omega_h} \\ &\quad + \theta_h \left\langle g_D \circ \boldsymbol{\eta}(\boldsymbol{\xi}) - T_h^k(u_I)|_{\boldsymbol{\eta}(\boldsymbol{\xi})}, v \right\rangle_{\Gamma_h} \quad \forall v \in V_h^k \end{aligned}$$

so that Lemma 9 implies the stability bound

$$(49) \quad \begin{aligned} \|w_h\|_{1,\Omega_h} &\leq C \left\{ \|\tilde{f} - [-\nabla \cdot (\tilde{p}\nabla u_I)]\|_{-1,\Omega_h} \right. \\ &\quad \left. + h^{-\frac{1}{2}} \|g_D \circ \boldsymbol{\eta}(\boldsymbol{\xi}) - T_h^k(u_I)|_{\boldsymbol{\eta}(\boldsymbol{\xi})}\|_{0,\Gamma_h} \right\}. \end{aligned}$$

Recalling that  $\hat{f} = L_D \tilde{u}$ , the first term on the right-hand side of (49) satisfies the bound

$$(50) \quad \|\tilde{f} - [-\nabla \cdot (\tilde{p}\nabla u_I)]\|_{-1,\Omega_h} \leq \|\tilde{f} - \hat{f}\|_{-1,\Omega_h} + \|\nabla \cdot [\tilde{p}\nabla(\tilde{u} - u_I)]\|_{-1,\Omega_h}.$$

From Lemma 7, we have that

$$\|\tilde{f} - \hat{f}\|_{-1,\Omega_h} = \sup_{\substack{\chi \in H_0^1(\Omega_h) \\ \|\chi\|_{1,\Omega_h}=1}} \left\langle \tilde{f} - \hat{f}, \chi \right\rangle_{\Omega_h} \leq \begin{cases} C_{k,d} \delta_h^{k-\frac{1}{2}} \|f\|_{k-1,\Omega} & \text{if } d=2, \\ C_{k,d} \delta_h^{k-1} \|f\|_{k-1,\Omega} & \text{if } d=3, \end{cases}$$

whereas standard interpolation theory implies that

$$\begin{aligned} \|\nabla \cdot [\tilde{p}\nabla(\tilde{u} - u_I)]\|_{-1,\Omega_h} &= \sup_{\substack{\chi \in H_0^1(\Omega_h) \\ \|\chi\|_{1,\Omega_h}=1}} -\langle \tilde{p}\nabla(\tilde{u} - u_I), \nabla \chi \rangle_{\Omega_h} \\ &\leq C \|\tilde{u} - u_I\|_{1,\Omega_h} \leq Ch^k \|u\|_{k+1,\Omega} \end{aligned}$$

after applying the extension bound, i.e.,  $\|\tilde{u}\|_{k+1,\Omega_h} \leq C\|u\|_{k+1,\Omega}$ . As a result,

$$(51) \quad \|\tilde{f} - [-\nabla \cdot (\tilde{p}\nabla u_I)]\|_{-1,\Omega_h} \leq Ch^k (\|u\|_{k+1,\Omega} + \|f\|_{k-1,\Omega}),$$

after recalling that  $\delta_h \sim o(h^{\frac{3}{2}})$  if  $d=2$  and  $\delta_h \sim O(h^2)$  if  $d=3$ .

We now take  $\delta_h \sim O(h^{\frac{3}{2}})$  for  $d=2,3$  to simplify the remainder of the proof. To estimate the second term on the right-hand side of (49) we first see that

$$\begin{aligned} &\|g_D \circ \boldsymbol{\eta}(\boldsymbol{\xi}) - T_h^k(u_I)|_{\boldsymbol{\eta}(\boldsymbol{\xi})}\|_{0,\Gamma_h} \\ &\leq \|g_D \circ \boldsymbol{\eta}(\boldsymbol{\xi}) - T_h^k(\tilde{u})|_{\boldsymbol{\eta}(\boldsymbol{\xi})}\|_{0,\Gamma_h} + \|T_h^k(\tilde{u} - u_I)|_{\boldsymbol{\eta}(\boldsymbol{\xi})}\|_{0,\Gamma_h}. \end{aligned}$$

By Lemma 2, we have that

$$\begin{aligned} \|g_D \circ \boldsymbol{\eta}(\boldsymbol{\xi}) - T_h^k(\tilde{u})|_{\boldsymbol{\eta}(\boldsymbol{\xi})}\|_{0,\Gamma_h} &= \|\tilde{u} \circ \boldsymbol{\eta}(\boldsymbol{\xi}) - T_h^k(\tilde{u})|_{\boldsymbol{\eta}(\boldsymbol{\xi})}\|_{0,\Gamma_h} \\ &\leq C_{\Omega_h} \delta_h^{k+\frac{1}{2}} |\tilde{u}|_{k+1,\mathbb{R}^N} \\ &\leq C_{\Omega_h} h^{\frac{3k}{2} + \frac{3}{4}} \|u\|_{k+1,\Omega}, \end{aligned}$$

after applying the assumption  $\delta \sim o(h^{\frac{3}{2}})$  in Theorem 1 and the extension bound. Additionally, let  $e_I = \tilde{u} - u_I$  be the interpolation error defined over  $\Omega_h$ . Then we have that

$$\|T_h^k(e_I)|_{\eta(\xi)}\|_{0,\Gamma_h} \leq \|T_h^k(e_I)|_{\eta(\xi)} - e_I\|_{0,\Gamma_h} + \|e_I\|_{0,\Gamma_h}.$$

By Lemma 3, we have that

$$\begin{aligned} \|T_h^k(e_I)|_{\eta(\xi)} - e_I\|_{0,\Gamma_h} &\leq C_{\Omega_h} \left( \delta_h^{\frac{1}{2}} \|e_I\|_{1,\Omega_h} + \delta_h^{k+\frac{1}{2}} \|e_I\|_{k+1,\Omega_h} \right) \\ &\leq C_{\Omega_h} \left( \delta_h^{\frac{1}{2}} h^k + \delta_h^{k+\frac{1}{2}} \right) \|u\|_{k+1,\Omega} \\ &\leq C_{\Omega_h} h^{k+\frac{3}{4}} \|u\|_{k+1,\Omega}, \end{aligned}$$

where we have again applied the assumption that  $\delta \sim o(h^{\frac{3}{2}})$  and the extension bound. Further, using the trace inequality

$$(52) \quad \|v\|_{0,\partial\mathcal{D}} \leq C \|v\|_{0,\mathcal{D}}^{\frac{1}{2}} \|v\|_{1,\mathcal{D}}^{\frac{1}{2}}$$

for  $v \in H^1(\mathcal{D})$  and  $\mathcal{D} \subset \mathbb{R}^N$  a Lipschitz domain [5, Theorem 1.6.6], we have that

$$\|e_I\|_{0,\Gamma_h} \leq C_{\Omega_h} \|e_I\|_{0,\Omega_h}^{\frac{1}{2}} \|e_I\|_{1,\Omega_h}^{\frac{1}{2}} \leq C_{\Omega_h} h^{k+\frac{1}{2}} \|u\|_{k+1,\Omega},$$

after applying the standard interpolation error bounds and extension bounds. Thus, from this analysis, we have that

$$(53) \quad \|g_D \circ \eta(\xi) - T_h^k(u_I)|_{\eta(\xi)}\|_{0,\Gamma_h} \leq Ch^{k+\frac{1}{2}} \|u\|_{k+1,\Omega}.$$

Combining (51) and (53) yields the optimal bound

$$(54) \quad \|w_h\|_{1,\Omega_h} \leq Ch^k \{ \|u\|_{k+1,\Omega} + \|f\|_{k-1,\Omega} \}$$

for the discrete error which completes the proof.  $\square$

**E.2. Proof of Theorem 4.** Our strategy is to couch the PE-FEM problem into a standard Dirichlet finite element formulation, under the additional assumption that  $u \in H^{k+\frac{3}{2}}(\Omega)$  and  $f \in H^k(\Omega)$  (and thus,  $\tilde{u} \in H^{k+\frac{3}{2}}(\mathbb{R}^N)$  and  $\tilde{f} \in H^k(\mathbb{R}^N)$ ), and then apply the well-known Aubin-Nitsche duality argument to the latter.

We begin with two technical lemmas.

**Lemma 10.** *Assume the hypotheses in Theorem 1, and in addition assume that  $u \in H^{k+\frac{3}{2}}(\Omega)$  and  $\delta_h \sim O(h^2)$ . Then, the trace of the discrete error  $(w_h)_* \in W_h^k$  satisfies the bound*

$$(55) \quad \|w_h\|_{0,\Gamma_h} \leq Ch^{k+1} (\|u\|_{k+1,\Omega} + |\tilde{u}|_{k+1,\Gamma_h} + \|f\|_{k-1,\Omega}).$$

*Proof.* First, we begin with a technical result that arises from the assumption that  $\tilde{u} \in H^{k+\frac{3}{2}}(\mathbb{R}^N)$  and  $\delta_h \sim O(h^2)$ . Under these assumptions we may modify the analysis on the  $\|g_D \circ \eta(\xi) - T_h^k(\tilde{u})|_{\eta(\xi)}\|_{0,\Gamma_h}$  term in the proof of Theorem 3 so that

$$(56) \quad \|g_D \circ \eta(\xi) - T_h^k(u_I)|_{\eta(\xi)}\|_{0,\Gamma_h} \leq Ch^{k+1} (\|u\|_{k+1,\Omega} + |\tilde{u}|_{k+1,\Gamma_h}).$$

This result is immediate after seeing that

$$\|\tilde{u} - u_I\|_{0,\Gamma_h} \leq Ch^{k+1} |\tilde{u}|_{k+1,\Gamma_h},$$

and taking  $\delta_h \sim O(h^2)$ .

From (18), we have that

$$w_h = \pi_h(g_D \circ \boldsymbol{\eta}(\boldsymbol{\xi}) - T_h^k(u_I)|_{\boldsymbol{\eta}(\boldsymbol{\xi})} - T_h^{1,k}(w_h)|_{\boldsymbol{\eta}(\boldsymbol{\xi})}),$$

where  $\pi_h : L^2(\Gamma_h) \rightarrow W_h^k$  is the  $L^2$  projection onto  $W_h^k$ . Using the continuity of  $\pi_h$  in  $L^2(\Gamma_h)$ , (56), Lemma 4, and (54), we have that

$$\begin{aligned} \|w_h\|_{0,\Gamma_h} &\leq C \left( \|g_D \circ \boldsymbol{\eta}(\boldsymbol{x}) - T_h^k(u_I)|_{\boldsymbol{\eta}(\boldsymbol{\xi})}\|_{0,\Gamma_h} + \left\| T_h^{1,k}(w_h)|_{\boldsymbol{\eta}(\boldsymbol{\xi})} \right\|_{0,\Gamma_h} \right) \\ &\leq C \left( h^{k+1} (\|u\|_{k+1,\Omega} + |\tilde{u}|_{k+1,\Gamma_h}) + \left\| T_h^{1,k}(w_h)|_{\boldsymbol{\eta}(\boldsymbol{\xi})} \right\|_{0,\Gamma_h} \right) \\ &\leq C \left( h^{k+1} (\|u\|_{k+1,\Omega} + |\tilde{u}|_{k+1,\Gamma_h}) + \sum_{|\boldsymbol{\alpha}|=1}^k h^{-|\boldsymbol{\alpha}|+\frac{1}{2}} \delta_h^{|\boldsymbol{\alpha}|} \|w_h\|_{1,\Omega_h} \right) \\ &\leq C \left( h^{k+1} (\|u\|_{k+1,\Omega} + |\tilde{u}|_{k+1,\Gamma_h}) + \sum_{|\boldsymbol{\alpha}|=1}^k h^{k+|\boldsymbol{\alpha}|+\frac{1}{2}} (\|u\|_{k+1,\Omega} + \|f\|_{k-1,\Omega}) \right) \\ &\leq Ch^{k+1} (\|u\|_{k+1,\Omega} + |\tilde{u}|_{k+1,\Gamma_h} + \|f\|_{k-1,\Omega}), \end{aligned}$$

thereby proving the result of this lemma.  $\square$

**Lemma 11.** Assume that  $u \in H^{k+\frac{3}{2}}(\Omega)$ ,  $\delta_h \sim O(h^2)$ , and that  $\phi_h \in V_h^k$  satisfies the conditions

$$\phi_h|_{\Gamma_h} = w_h, \quad \sup_{\boldsymbol{x} \in \Omega_h} |\phi_h| = \sup_{\boldsymbol{\xi} \in \Gamma_h} |w_h|, \quad \text{and} \quad \phi_h = 0 \text{ over } \Omega_h^0,$$

where  $\Omega_h^0 := \{\boldsymbol{x} \in \mathcal{K}_n : \mathcal{K}_n \cap \Gamma_h = \emptyset\}$ . Then,

$$\|\phi_h\|_{0,\Omega_h} \leq Ch^{k+\frac{3}{2}} (\|u\|_{k+1,\Omega} + |\tilde{u}|_{k+1,\Gamma_h} + \|f\|_{k-1,\Omega}).$$

*Proof.* Let  $\Omega_h^b := \Omega_h \setminus \Omega_h^0$ . Because  $\phi_h = 0$  on  $\Omega_h^0$ , the inverse inequality implies

$$\begin{aligned} \|\phi_h\|_{0,\Omega_h}^2 &= \sum_{\mathcal{K}_n \in \Omega_h^b} \|\phi_h\|_{0,\mathcal{K}_n}^2 \leq \sum_{\mathcal{K}_n \in \Omega_h^b} Ch^d \|\phi_h\|_{L^\infty(\mathcal{K}_n)}^2 \\ &= \sum_i Ch^d \|w_h\|_{L^\infty(\mathcal{E}_i)}^2 \leq \sum_i Ch \|w_h\|_{0,\mathcal{E}_i}^2 = Ch \|w_h\|_{0,\Gamma_h}^2. \end{aligned}$$

The proof follows by an application of Lemma 10.  $\square$

We proceed with the main result.

*Proof of Theorem 4.* We couch the PE-FEM Dirichlet problem into an equivalent standard FEM Dirichlet problem as follows. Then, for the extension  $\tilde{u}$ , we have that  $\tilde{u} \in H^1(\Omega_h)$  satisfies

$$D_h(\tilde{u}, v) = \left\langle \hat{f}, v \right\rangle_{\Omega_h} \quad \forall v \in H_0^1(\Omega_h).$$

Let  $\phi_h \in V_h^k$  denote a function satisfying the hypothesis of Lemma 11. Then it is not difficult to see that the solution  $u_h \in V_h^k$  of the Dirichlet PE-FEM problem (18) is also a solution to the following weak problem: seek  $u_h \in V_{h,0}^k + u_I + \phi_h$  such that

$$D_h(u_h, v) = \left\langle \tilde{f}, v \right\rangle_{\Omega_h} \quad \forall v \in V_{h,0}^k,$$

where  $u_I \in V_h^k$  denotes the interpolant of  $\tilde{u}$  over  $\Omega_h$ . These results imply that

$$(57) \quad D_h(\tilde{u} - u_h, v) = \left\langle \hat{f} - \tilde{f}, v \right\rangle_{\Omega_h} \quad \forall v \in V_{h,0}^k.$$

Let  $u_h^0 = u_h - u_I - \phi_h$ , and consider the following continuous and discrete dual problems: seek  $\psi \in H_0^1(\Omega_h)$  such that

$$(58) \quad D_h(\chi, \psi) = (u_h^0, \chi)_{\Omega_h} \quad \forall \chi \in H_0^1(\Omega_h)$$

and  $\psi_h \in V_{h,0}^k$  such that

$$(59) \quad D_h(\chi, \psi_h) = (u_h^0, \chi)_{\Omega_h} \quad \forall \chi \in V_{h,0}^k.$$

Under the assumptions made on the domain in the statement of the theorem, we have that (58) satisfies the following continuity bound on polytopal domains [16, 20]:

$$(60a) \quad \|\psi\|_{1+s, \Omega_h} \leq C \|u_h^0\|_{0, \Omega_h},$$

where  $s \in (\frac{1}{2}, 1]$  is a constant dependent on the largest interior angle of  $\partial\Omega_h$ . If all interior angles are bounded above by  $\pi$  we have that  $s = 1$ . We also have that the solution of (59) satisfies

$$(60b) \quad \|\psi_h\|_{1, \Omega_h} \leq C \|u_h^0\|_{-1, \Omega_h}.$$

Combining these results with standard finite element error bounds obtained from Céa's lemma allows us to conclude that

$$(60c) \quad \|\psi - \psi_h\|_{1, \Omega_h} \leq Ch^s |\psi|_{1+s, \Omega_h} \leq Ch^s \|u_h^0\|_{0, \Omega_h}.$$

Applying Lemmas 7 and 11 together with standard interpolation results, (57), (60a), and (60b) yield

$$\begin{aligned} \|u_h^0\|_{0, \Omega_h}^2 &= D_h(u_h^0, \psi) = D_h(u_h, \psi) - D_h(u_I + \phi_h, \psi) \\ &= D_h(u_h - \tilde{u}, \psi) - D_h(u_I - \tilde{u} + \phi_h, \psi) \\ &= D_h(u_h - \tilde{u}, \psi - \psi_h) + D_h(u_h - \tilde{u}, \psi_h) - D_h(u_I - \tilde{u} + \phi_h, \psi) \\ &= D_h(u_h - \tilde{u}, \psi - \psi_h) + \left\langle \tilde{f} - \hat{f}, \psi_h \right\rangle_{\Omega_h} - \left\langle u_I - \tilde{u} + \phi_h, u_h^0 \right\rangle_{\Omega_h} \\ &\quad - \left\langle u_I - \tilde{u} + \phi_h, \tilde{p} \nabla \psi \cdot \mathbf{n}_h \right\rangle_{\Gamma_h} \\ &\leq C \left( \|\tilde{u} - u_h\|_{1, \Omega_h} \|\psi - \psi_h\|_{1, \Omega_h} + \|\tilde{f} - \hat{f}\|_{-1, \Omega_h} \|\psi_h\|_{1, \Omega_h} \right. \\ &\quad \left. + (\|\tilde{u} - u_I\|_{0, \Omega_h} + \|\tilde{u} - u_I\|_{0, \Gamma_h} + \|\phi_h\|_{0, \Omega_h} + \|\phi_h\|_{0, \Gamma_h}) \|u_h^0\|_{0, \Omega_h} \right) \\ &\leq Ch^{k+s} (\|u\|_{k+1, \Omega_h} + |\tilde{u}|_{k+1, \Gamma_h} + \|f\|_{k, \Omega_h}) \|u_h^0\|_{0, \Omega_h}, \end{aligned} \quad (61)$$

after seeing that

$$\begin{aligned} D_h(u_I - \tilde{u} + \phi_h, \psi) &:= \int_{\Omega_j} \tilde{p} \nabla (u_I - \tilde{u} + \phi_h) \cdot \nabla \psi d\mathbf{x} \\ &= \int_{\Omega_h} (u_I - \tilde{u} + \phi_h) L_D \psi d\mathbf{x} + \int_{\Gamma_h} (u_I - \tilde{u} + \phi_h) \tilde{p} \nabla \psi \cdot \mathbf{n}_h ds \end{aligned}$$

from Green's identity, recalling that  $L_D\psi = u_h^0$ , and subsequently having that

$$\begin{aligned} \langle u_I - \tilde{u} + \phi_h, \tilde{p}\nabla\psi \cdot \mathbf{n}_h \rangle_{\Gamma_h} &\leq \bar{p} (\|u_I - \tilde{u}\|_{1/2-s, \Gamma_h} + \|\phi_h\|_{1/2-s, \Gamma_h}) \|\nabla\psi\|_{s-1/2, \Gamma_h} \\ &\leq \bar{p} (\|u_I - \tilde{u}\|_{0, \Gamma_h} + \|\phi_h\|_{0, \Gamma_h}) \|\psi\|_{1+s, \Omega_h}. \end{aligned}$$

Here, the trace is well-defined since we have taken  $s > \frac{1}{2}$  (see Remark 8). To complete the proof we use the above result in conjunction with the triangle inequality to obtain

$$\|\tilde{u} - u_h\|_{0, \Omega_h} \leq \|u_h^0\|_{0, \Omega_h} + \|\tilde{u} - u_I\|_{0, \Omega_h} + \|\phi_h\|_{0, \Omega_h}$$

from which the result of the theorem follows after applying (61), standard interpolation bounds, and Lemma 11.  $\square$

*Remark 8.* Because we have assumed that  $\Gamma$  is  $C^{k+1}$  smooth, there exists an  $h_0$  such that for all  $h < h_0$  we have that the largest interior angle of  $\Gamma_h$  is bounded above by  $\frac{3\pi}{2}$ . This implies that  $\psi \in H^{1+s}(\Omega_h)$  with  $s > \frac{1}{2}$ . Additionally, because the largest interior angle of  $\Gamma_h$  approaches  $\pi$  as  $h \rightarrow 0$ , we have that  $s \rightarrow 1$  as  $h \rightarrow 0$ . Therefore the  $L^2$  estimate presented above for nonconvex polytopal domains is asymptotically optimal.

**E.3. Proof of Theorem 5.** We assume that (6) has a solution  $u \in H^{k+1}(\Omega)$  with an extension  $\tilde{u} \in H^{k+1}(\mathbb{R}^N)$ . We denote  $\hat{f} = L_N \tilde{u}$ , where  $L_N$  is the strong operator in (4). It follows that  $\tilde{u}$  satisfies

$$(62) \quad N_h(\tilde{u}, v_h) - \langle \tilde{p}\nabla\tilde{u} \cdot \mathbf{n}_h, v_h \rangle_{\Gamma_h} = \left\langle \hat{f}, v_h \right\rangle_{\Omega_h} \quad \forall v_h \in V_h^k(\Omega_h).$$

From the derivation of Strang's lemma [5, Theorem 10.1.1], we have that

$$(63) \quad \begin{aligned} \|\tilde{u} - u_h\|_{1, \Omega_h} &\leq C_1 \inf_{w \in V_h^k} \left[ \|\tilde{u} - w\|_{1, \Omega_h} \right. \\ &\quad \left. + \sup_{\substack{v \in V_h^k \\ \|v\|_{1, \Omega_h} = 1}} \left( |B_{h,N}(\tilde{u} - w, v)| + |B_{h,N}(\tilde{u}, v) - F_{h,N}(v)| \right) \right]. \end{aligned}$$

Setting  $w = u_I$ , where  $u_I \in V_h^k$  is the Lagrange interpolant of  $\tilde{u}$ , we have, by (33) and standard interpolation bounds and recalling that we have now required that  $\delta_h \leq Ch^2$ , that

$$(64) \quad \sup_{\substack{v \in V_h^k \\ \|v\|_{1, \Omega_h} = 1}} |B_{h,N}(\tilde{u} - w, v)| \leq Ch^k |u|_{k+1, \Omega_h}.$$

From the definition of  $B_{h,N}$  and (62), we have

$$B_{h,N}(\tilde{u}, v) = \left\langle \hat{f}, v \right\rangle_{\Omega_h} + \left\langle \tilde{p} \circ \boldsymbol{\eta}(\boldsymbol{\xi}) \mathbf{T}_h^{k-1}(\nabla\tilde{u})|_{\boldsymbol{\eta}(\boldsymbol{\xi})} \cdot \mathbf{n}, v \right\rangle_{\Gamma_h}.$$

Recalling (17) we have that

$$B_{h,N}(\tilde{u}, v) = \left\langle \hat{f}, v \right\rangle_{\Omega_h} + \left\langle g_N \circ \boldsymbol{\eta}(\boldsymbol{\xi}) - \tilde{p} \circ \boldsymbol{\eta}(\boldsymbol{\xi}) \mathbf{R}_h^{k-1}(\nabla\tilde{u})|_{\boldsymbol{\eta}(\boldsymbol{\xi})} \cdot \mathbf{n}, v \right\rangle_{\Gamma_h}.$$

Thus, we have from Lemmas 2 and 7 that

$$\begin{aligned}
 & \sup_{\substack{v \in V_h^k \\ \|v\|_{1,\Omega_h} = 1}} |B_{h,N}(\tilde{u}, v) - F_{h,N}(v)| \\
 (65) \quad &= \sup_{\substack{v \in V_h^k \\ \|v\|_{1,\Omega_h} = 1}} \left| \left\langle \hat{f} - \tilde{f}, v \right\rangle_{\Omega_h} - \left\langle \tilde{p} \circ \boldsymbol{\eta}(\boldsymbol{\xi}) \mathbf{R}_h^{k-1}(\nabla \tilde{u})|_{\boldsymbol{\eta}(\boldsymbol{\xi})} \cdot \mathbf{n}, v \right\rangle_{\Gamma_h} \right| \\
 &\leq C \delta_h^{k-1} \|f\|_{k-1,\Omega} + C \delta_h^{k+\frac{1}{2}} |u|_{k+1,\Omega} \leq Ch^k (\|f\|_{k-1,\Omega} + |u|_{k+1,\Omega}).
 \end{aligned}$$

The result of the theorem follows by inserting (64) and (65) into (63) and subsequently applying the approximation bound (2).

## REFERENCES

- [1] R. A. Adams and J. J. F. Fournier, *Sobolev Spaces*, 2nd ed., Pure and Applied Mathematics (Amsterdam), vol. 140, Elsevier/Academic Press, Amsterdam, 2003. MR2424078
- [2] J. W. Barrett and C. M. Elliott, *Finite element approximation of the Dirichlet problem using the boundary penalty method*, Numer. Math. **49** (1986), no. 4, 343–366, DOI 10.1007/BF01389536. MR853660
- [3] L. Beirão Da Veiga, A. Russo, and G. Vacca, *The virtual element method with curved edges*, arXiv preprint (2018).
- [4] P. B. Bochev and M. D. Gunzburger, *Least-Squares Finite Element Methods*, Applied Mathematical Sciences, vol. 166, Springer, New York, 2009. MR2490235
- [5] S. C. Brenner and L. R. Scott, *The Mathematical Theory of Finite Element Methods*, 3rd ed., Texts in Applied Mathematics, vol. 15, Springer, New York, 2008. MR2373954
- [6] E. Burman, P. Hansbo, and M. G. Larson, *A cut finite element method with boundary value correction*, Math. Comp. **87** (2018), no. 310, 633–657, DOI 10.1090/mcom/3240. MR3739212
- [7] J. Cheung, M. Perego, and P. Bochev, *New developments in using Schwarz methods for model coupling*, in Center for Computing Research Summer Proceedings 2015, A. M. Bradley and M. L. Parks, eds., Technical Report SAND2016-0830R, Sandia National Laboratories, 2015, pp. 14–26.
- [8] J. Cheung, M. Perego, P. Bochev, and M. Gunzburger, *An optimally convergent coupling approach for interface problems approximated with higher-order finite elements*, arXiv preprint (2017).
- [9] P. G. Ciarlet, *The Finite Element Method for Elliptic Problems*, Classics in Applied Mathematics, vol. 40, Society for Industrial and Applied Mathematics (SIAM), Philadelphia, PA, 2002. Reprint of the 1978 original [North-Holland, Amsterdam; MR0520174 (58 #25001)]. MR1930132
- [10] P. G. Ciarlet, *Linear and Nonlinear Functional Analysis with Applications*, Society for Industrial and Applied Mathematics, Philadelphia, PA, 2013. MR3136903
- [11] P. G. Ciarlet and P.-A. Raviart, *Interpolation theory over curved elements, with applications to finite element methods*, Comput. Methods Appl. Mech. Engrg. **1** (1972), 217–249, DOI 10.1016/0045-7825(72)90006-0. MR0375801
- [12] B. Cockburn, W. Qiu, and M. Solano, *A priori error analysis for HDG methods using extensions from subdomains to achieve boundary conformity*, Math. Comp. **83** (2014), no. 286, 665–699, DOI 10.1090/S0025-5718-2013-02747-0. MR3143688
- [13] B. Cockburn and M. Solano, *Solving Dirichlet boundary-value problems on curved domains by extensions from subdomains*, SIAM J. Sci. Comput. **34** (2012), no. 1, A497–A519, DOI 10.1137/100805200. MR2890275
- [14] B. Cockburn and M. Solano, *Solving convection-diffusion problems on curved domains by extensions from subdomains*, J. Sci. Comput. **59** (2014), no. 2, 512–543, DOI 10.1007/s10915-013-9776-y. MR3188451
- [15] J. A. Cottrell, T. J. R. Hughes, and Y. Bazilevs, *Isogeometric Analysis: Toward Integration of CAD and FEA*, John Wiley & Sons, Ltd., Chichester, 2009. MR3618875

- [16] M. Dauge, *Elliptic Boundary Value Problems on Corner Domains: Smoothness and Asymptotics of Solutions*, Lecture Notes in Mathematics, vol. 1341, Springer-Verlag, Berlin, 1988. MR961439
- [17] I. Ergatoudis, B. Irons, and O. Zienkiewicz, *Curved, isoparametric, quadrilateral elements for finite element analysis*, Internat. J. Solids and Structures **4** (1968), 31–42.
- [18] A. Ern and J.-L. Guermond, *Theory and Practice of Finite Elements*, Applied Mathematical Sciences, vol. 159, Springer-Verlag, New York, 2004. MR2050138
- [19] I. Fried, *Accuracy and condition of curved (isoparametric) finite elements*, J. Sound and Vibration **31** (1973), 345–355.
- [20] P. Grisvard, *Elliptic Problems in Nonsmooth Domains*, Classics in Applied Mathematics, vol. 69, Society for Industrial and Applied Mathematics (SIAM), Philadelphia, PA, 2011. Reprint of the 1985 original [MR0775683]; With a foreword by Susanne C. Brenner. MR3396210
- [21] T. J. R. Hughes, J. A. Cottrell, and Y. Bazilevs, *Isogeometric analysis: CAD, finite elements, NURBS, exact geometry and mesh refinement*, Comput. Methods Appl. Mech. Engrg. **194** (2005), no. 39–41, 4135–4195, DOI 10.1016/j.cma.2004.10.008. MR2152382
- [22] L. Krivodonova and M. Berger, *High-order accurate implementation of solid wall boundary conditions in curved geometries*, J. Comput. Phys. **211** (2006), no. 2, 492–512, DOI 10.1016/j.jcp.2005.05.029. MR2173394
- [23] M. Lenoir, *Optimal isoparametric finite elements and error estimates for domains involving curved boundaries*, SIAM J. Numer. Anal. **23** (1986), no. 3, 562–580, DOI 10.1137/0723036. MR842644
- [24] A. Main and G. Scovazzi, *The shifted boundary method for embedded domain computations. Part I: Poisson and Stokes problems*, J. Comput. Phys. **372** (2018), 972–995, DOI 10.1016/j.jcp.2017.10.026. MR3847465
- [25] A. Main and G. Scovazzi, *The shifted boundary method for embedded domain computations. Part II: Linear advection-diffusion and incompressible Navier-Stokes equations*, Internat. J. Solids and Structures, to appear.
- [26] F. J. Narcowich, J. D. Ward, and H. Wendland, *Sobolev bounds on functions with scattered zeros, with applications to radial basis function surface fitting*, Math. Comp. **74** (2005), no. 250, 743–763, DOI 10.1090/S0025-5718-04-01708-9. MR2114646
- [27] R. Sevilla, S. Fernández-Méndez, and A. Huerta, *NURBS-enhanced finite element method (NEFEM). A seamless bridge between CAD and FEM*, Arch. Comput. Methods Eng. **18** (2011), no. 4, 441–484, DOI 10.1007/s11831-011-9066-5. MR2851386
- [28] G. Strang and G. J. Fix, *An Analysis of the Finite Element Method*, Prentice-Hall Series in Automatic Computation, Prentice-Hall, Inc., Englewood Cliffs, N. J., 1973. MR0443377
- [29] Z. Zhang and A. Naga, *A new finite element gradient recovery method: superconvergence property*, SIAM J. Sci. Comput. **26** (2005), no. 4, 1192–1213, DOI 10.1137/S1064827503402837. MR2143481
- [30] O. Zienkiewicz, R. Taylor, and R. Taylor, *The Finite Element Method*, McGraw-Hill, London, 1977.

INTERDISCIPLINARY CENTER FOR APPLIED MATHEMATICS, VIRGINIA TECH, BLACKSBURG, VIRGINIA 24061

*Email address:* jamescheung@vt.edu

CENTER FOR COMPUTING RESEARCH, SANDIA NATIONAL LABORATORIES, ALBUQUERQUE, NEW MEXICO 87123

*Email address:* mperego@sandia.gov

CENTER FOR COMPUTING RESEARCH, SANDIA NATIONAL LABORATORIES, ALBUQUERQUE, NEW MEXICO 87123

*Email address:* pboche@sandia.gov

DEPARTMENT OF SCIENTIFIC COMPUTING, FLORIDA STATE UNIVERSITY, TALLAHASSEE, FLORIDA 32309

*Email address:* mgunzburger@fsu.edu